

Superconductivity Web21

Published by International Superconductivity Technology Center
1-10-13 Shinonome Koto-ku, Tokyo 135-0062, Japan Tel:+81-3-3536-7283, Fax:+81-3-3536-5717

Contents:

Topics

- Brief Summary of the IEC-TC90 Conference held in Xian, China
- Wind Heat Power (WHP)
- What's New in the World of Superconductivity (November, 2012)

Feature Articles: SQUID Applications

- Utilizing HTS-SQUID for Non-destructive Testing Evaluating The Destructive Mechanism of Braided CFRPs
- Development of a Compact Magnetometer Using HTS-SQUID and a Rotating Sample
- Development of A Biological Immunoassays Employing Magnetic Markers (HTS-SQUID)
- A Large-scale Magnetic Field Gradiometer Utilizing YBCO High Temperature Superconducting Tapes
- Realizing A SQUID Magnetometer for Practical Geomagnetic Field Measurements
- Ultra-low-Field NMR Measurements of Protons and Fluorine Nuclei using SQUID
- The Current Status of SQUID-Readout Development for Superconducting Detectors in Japan

Feature Article: Superconducting Digital Devices (Low Temperature)

- Trends in Superconducting Digital Device Technology
- The Fabrication Process Development of Small Al/AIO_x/Al Trilayer Josephson Junctions
- High Speed Operations of a Superconducting Flash A/D Converter in a Cryocooler System (movie)
- Investigation of Adiabatic QFP Logic Circuits with Extremely Low Power Consumption
- Measurement of an SFQ Time to Digital Converter for Mass Spectrometry
- Low-jitter Signal Readout from SSPD Utilizing A SFQ Circuit
- Success in a Principle Experiment Related to Quantum Memory – Advancement towards The Realization of A Quantum Computer

[Top of Superconductivity Web21](#)

Superconductivity Web21

Published by International Superconductivity Technology Center

1-10-13 Shinonome, Koto-ku, Tokyo 135-0062, Japan

Tel: +81-3-3536-7283 Fax: +81-3-3536-5717

Top of Superconductivity Web21: <http://www.istec.or.jp/web21/web21-E.html>



This work was subsidized by JKA using promotion funds from

KEIRIN RACE

<http://ringing-keirin.jp>



Superconductivity Web21

Published by International Superconductivity Technology Center
1-10-13, Shinonome, Koto-ku, Tokyo 135-0062, Japan T el: +81-3-3536-7283, Fax: +81-3-3536-5717

Topics: Brief Summary of the IEC-TC90 Conference held in Xian, China

Ryohei Kondo,
Managing Director, ISTECC
IEC-TC90 Japanese National Committee

The International Electrotechnical Commission (IEC), an international organization involved in the development and publishing of international standards regarding electrical and electronic engineering, held its TC90 conference on superconductivity at the Bell Tower Hotel in Xi'an, China on 20th-22nd August. The conference, attended by 34 participants from six countries held their working group (WG) sub-committee meetings. A mini symposium to deepen mutual understandings was held on the second day of the conference followed by the TC90 plenary on the final day.

Participants from six countries attended the TC90 plenary – three secretariat members (chaired by Dr. Bruzek from France), Japan (9 members including Teruo Matsushita, Professor Emeritus of Kyushu Institute of Technology as Chair of Japanese National Committee of IEC/TC90), China (11 members), Korea (5 members), Germany (2 members) and USA (2 members). The IEC Central Office also participated in the meeting actively exchanging their opinions. The following account briefly reports on the plenary meeting regarding the results and outcomes from WG and mini symposium.



Bell Tower Hotel Xi'an and South Street, as seen from the Bell Tower.

<References>

- IEC was founded in 1906, with Japan formally joining the organization in 1910. Currently, regular members from 60 countries and associate members in 22 countries are members of the organization, with a total of 175 Technical Committees (TC) and Sub Committees (SC).
- TC90 was founded in 1989 and is held every other year in order to facilitate discussions of international standards regarding superconducting materials and equipment. Ten countries participate in TC90, with Japan being the secretariat. (Mr. Kenichi Sato, a Fellow of Sumitomo Electric Industries, Ltd. as International Secretary of IEC/TC90)

Superconductivity Web21

Published by International Superconductivity Technology Center
1-10-13, Shinonome, Koto-ku, Tokyo 135-0062, Japan T el: +81-3-3536-7283, Fax: +81-3-3536-5717

IEC trends

- Mr. Sebellin, from the IEC Central Office, proposed that the Committee Draft for Voting (CDV) be shortened to three months (usually five months). He also inferred to the trends of recent discussions, which seem to focus on smart grid and renewable energy.

Drafting the standards and revision status

- 16 standards related to superconductor-related vocabulary and measurement methods have already been published. 14 WGs were established at TC90. Amongst these, eight WGs and one ad-hoc group held subcommittee meetings, discussing recent developments as well as future courses of action. Japanese participants acted as conveners for all groups (some were convened with cooperation of overseas members).

- Some draft standards were reassessed and a revised date agreed. For example, the following were agreed at the meeting; New Work Item Proposal (NWIP) to be extended for an additional two years, which pertains to I_c characteristics of Bi-2223 superconducting wires under bending conditions. A Round Robin Test (RRT) measuring REBCO wire I_c characteristics to be launched within a year after establishing testing method guidelines. Preparing a 2013 guideline pertaining to tensile strength measurements of BSCCO and REBCO wires at 77 K. Additionally, an extension of the CDV target period to April 2014 for two general rules proposed, relating to the general characteristics of superconducting wires, and reassessing the Committee Draft (CD) from the viewpoint of buyer and manufacturer.

- Additionally, the following were agreed at the meeting. The measurement methods undertaken to determine Residual Resistivity Ratio (RRR) of Nb-Ti and Nb₃Sn wires to be integrated in the next edition, and further investigation on Matrix Composition Ratio techniques, utilizing image processing for the measurements of MgB₂ and BSCCO composite superconductors to be discussed at the next meeting.

- The meeting declared that NWIP relating to a superconducting sensor would be submitted during 2013.



Plenary meeting scene

Any other business

- Discussions were held on strengthening cooperation and relationships with working groups on International Council On Large Electric Systems (CIGRE), who undertake technical investigations into superconducting equipment, in addition to TC20, who perform power cable-related standardization.

Superconductivity Web21

Published by International Superconductivity Technology Center
1-10-13, Shinonome, Koto-ku, Tokyo 135-0062, Japan T el: +81-3-3536-7283, Fax: +81-3-3536-5717

- The next TC90 meeting is planned around June-time, in Paris, two years from now.

- The author attended the IEC/TC90 conference for the first time. It is his opinion that Asian groups are making efforts in both R&D activities and superconductivity standardization, whereas Europe and USA are trying to lead standardization. The author realizes the significance of holding the IEC/TC90 overseas with Japan taking the initiative.

The author expresses his gratitude to the Japanese participants who extended their efforts in being secretariats of IEC/TC90 and also leading each WG. The author also expresses his thanks to all the Chinese members who prepared and welcomed us politely, hoping that via various routes, including R&D activities will foster sustainable peaceful relationships between Japan and China.

(Published in a Japanese version in the October 2012 issue of *Superconductivity Web 21*)

[Top of Superconductivity Web21](#)

Superconductivity Web21

Published by International Superconductivity Technology Center
1-10-13, Shinonome, Koto-ku, Tokyo 135-0062, Japan Tel: +81-3-3536-7283, Fax: +81-3-3536-5717

Topics: Wind Heat Power (WHP)

Toru Okazaki, Director
Public Relations Division/International Affairs Division
ISTEC

The output supply of power generated by wind and other forms of natural energy has issues with instability. Additionally, noise is also an issue. Wind Heat Power (WHP) is perceived as being able to overcome such issues. A presentation, entitled "Wind Heat Power", was positively acknowledged and appraised at the Joint Technical Meeting on Power Engineering and Power Systems Engineering of the Institute of Electrical Engineers of Japan. The following provides key excerpts. Superconductors applied to this technology would enable the realization of greater cost reductions as well as stable power generation at costs lower than currently available methods.

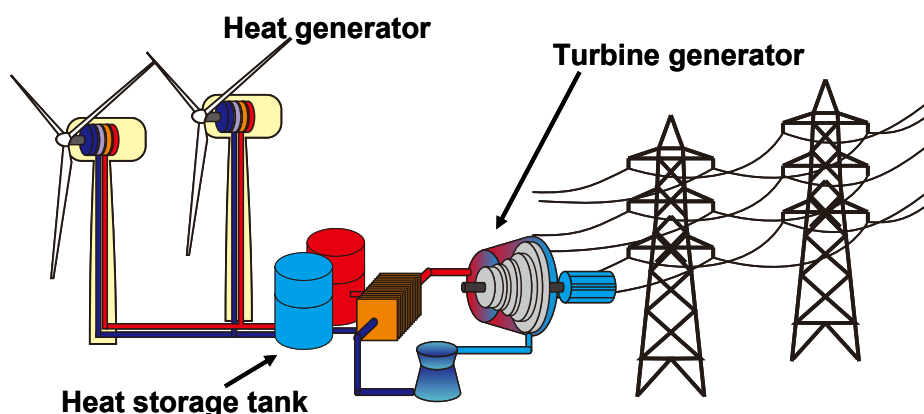


Fig.1 Schematic of Wind Heat Power

Figure 1 shows a schematic of the WHP. The installation of a so-called heat generator – a type of electric brake that utilizes eddy currents in the upper portion of a wind tower, allows the direct conversion of rotational energy to thermal energy. Since a form of electrical energy does not produce the power output, a lightweight and low-cost heat generator is possible. Thermal oils and molten salts transports the heat generated to heat storage tanks on the ground, allowing the stored heat to be utilized to generate electricity using a steam turbine whenever necessary. The latter has been utilized the same way in recent years for a solar-power tower, enabling more stable power generation than solar photovoltaics. This may at first seem to be less efficient and lack the benefits compared to conventional wind power generation, however **quantitative studies have concluded from the point of view of efficiency and maintenance that this method produces the lowest energy cost.** Some reasons are listed here:

1. Introducing current forms of natural energy is not feasible without the installation of more state-of-art thermal power plants.
2. Introduction of large-scale natural energy resources requires control of the power output generated (entire energy purchase is impossible).

Superconductivity Web21

Published by International Superconductivity Technology Center
 1-10-13, Shinonome, Koto-ku, Tokyo 135-0062, Japan Tel: +81-3-3536-7283, Fax: +81-3-3536-5717

3. The high costs of wind turbine generators are prohibitive.
4. Electricity storage systems so far reported, have yet to be sought for possible installation at power supply sites.

The author plans to provide detailed information on the above in future Web21 articles (a series of articles every other month is planned for 2013). Figure 2 shows an electricity cost comparison assuming a stable power supply. The cost of Wind Heat Power, referred to as WHP, is compared to the cost of other forms of energies when combined with current technologies, including optimized WHP, which takes into account its associated developmental factors. Comparisons were made based upon an EU performance base, with the results showing that energy costs are cheaper compared to the current status of Japan, but still more expensive compared to the current status of China. However, **if a superconducting heat generator is utilized in WHP, then lower energy costs than those described in figure 2 are expected.**

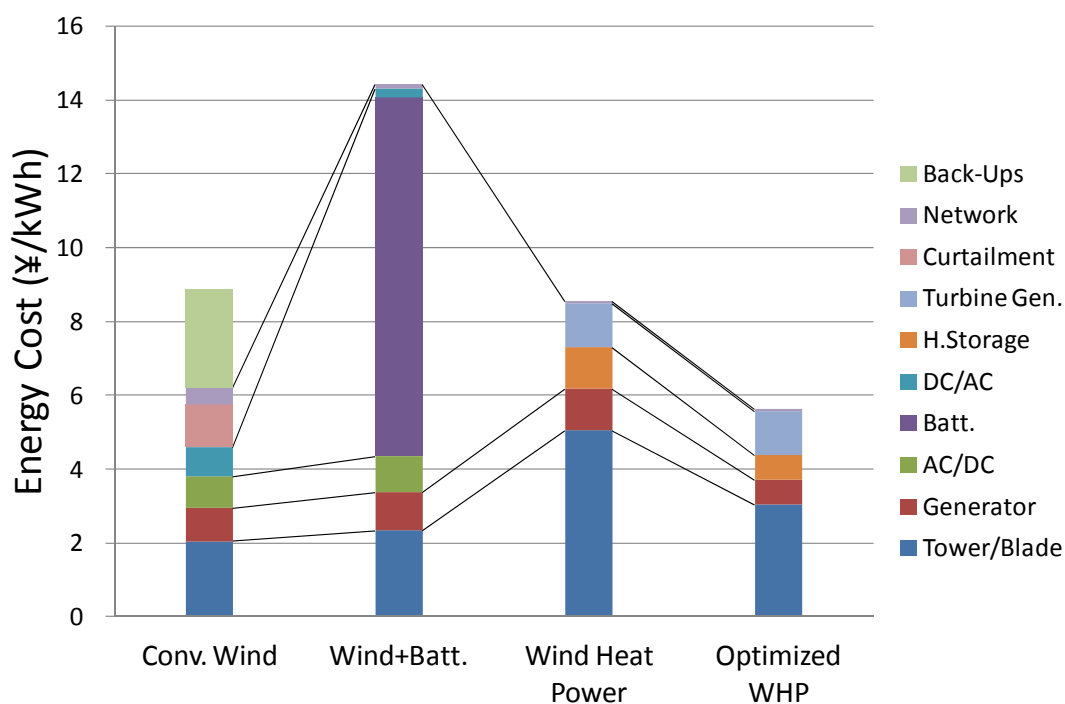


Fig. 2 Cost estimate results (in case of normal conducting)

Large losses typically occur when thermal energy is converted to kinetic energy. However, greater efficiencies can be realized by increasing operating gas temperatures. Heat generators produce heat using the principle of eddy currents, and operating temperatures can be increased to the point where metals can melt. Nevertheless, there are not many metals that sustain magnetic properties at such high temperatures, and in fact, a strong magnetomotive force is required here. A superconductor is therefore required for heat generators operating at much higher temperatures, just the same way as a superconductor is required for MRI, which forms strong magnetic fields spatially. It is expected that the heat-generator system cost forms a small part of the entire system cost and the application of a superconductor does not impact overall costs, and with efficiency expected to improve 1.5 – 2 times, leads to the possibility of significant reductions in energy costs. At present, there are few heat generator application examples and the possibility of a

Superconductivity Web21

Published by International Superconductivity Technology Center
1-10-13, Shinonome, Koto-ku, Tokyo 135-0062, Japan Tel: +81-3-3536-7283, Fax: +81-3-3536-5717

normal-conducting heat generator operating at high temperatures cannot be ignored completely. However, it is possible to state that only superconductors allow the realization of a high temperature system applicable to currently available heat generators.

Such superconducting-based heat generators can be considered for other applications since their temperature can be increased to the point where metals melt. For example, when the temperature is raised to nearly 1000°C, high temperature water vapor electrolysis, energy storage by hydrogen production, and potential coal gasification processing methods can be made possible, thus opening the door to an array of technology facilitated by employing superconductors.

The concept of this WHP itself is quite new. It is therefore important that many permutations are attempted. In particular, it is imperative to be aware of the fact that wind power generation is a comprehensive technology requiring consideration on its location, method, constructional element, procurement, transportation, construction, operation etc. There are no major issues for the realization of WHP, however there are potentially two electrical equipment and thermo mechanics aspects that need to be optimized, but are difficult to establish. The author considers it important to launch full-scale development by, first of all, undertaking a wide range of investigations, prototype fabrication and testing.

(Published in a Japanese version in the November 2012 issue of *Superconductivity Web 21*)

[Top of Superconductivity Web21](#)

Superconductivity Web21

Published by International Superconductivity Technology Center
1-10-13, Shinonome, Koto-ku, Tokyo 135-0062, Japan Tel: +81-3-3536-7283, Fax: +81-3-3536-5717

What's New in the World of Superconductivity (November, 2012)

초전도 뉴스 -세계의 동향-

超电导新闻 -世界的动向-

chāo diàn dǎo xīnwén - shìjiè de dòngxiàng-

Yutaka Yamada, Principal Research Fellow
Superconductivity Research Laboratory, ISTECC



★News sources and related areas in this issue

▶Power Application 전력응용 电力应用 [diànlì yìngyòng]



Superconducting FCL Launched with Nexans

AMSC (December 5, 2012)

AMSC and Nexans have introduced a medium-voltage superconductor fault current limiter (SFCL) to the North American market. SFCLs are expected to be a cost-effective solution to the growing challenge caused by fault currents. The SFCL offered by AMSC and Nexans is an extremely fast (with a response time of less than 2 ms) and self-acting, passive system that limits fault currents to safe, manageable levels.

Superconductivity Web21

Published by International Superconductivity Technology Center
1-10-13, Shinonome, Koto-ku, Tokyo 135-0062, Japan Tel: +81-3-3536-7283, Fax: +81-3-3536-5717

SFCL systems with ratings of up to 36 kV will be made available, which should allow their use in most utility distribution systems. By lowering peak currents during faults, electric utilities can expect to greatly reduce system equipment costs, defer or eliminate equipment replacement, increase equipment life expectancy, improve grid performance and operation, simplify the integration of renewable energy sources into the grid, and improve operator safety. SFCL systems have already been installed in Germany and the United Kingdom, and additional installations are planned in Europe. Daniel P. McGahn, AMSC President and Chief Executive Officer, commented, "We are pleased to be expanding our product line and our relationship with Nexans with the launch of the SFCL. Having successfully teamed to install superconductor power cables and develop and demonstrate SFCL systems, both AMSC and Nexans believe the time is now to begin capitalizing on the tremendous potential that exists for these offerings in the utility market."

Source: "Nexans and AMSC Introduce Fault Current Limiter for North American Utilities"

AMSC press release (December 5, 2012)

URL:

http://files.shareholder.com/downloads/AMSC/1729988020x0x620122/f090f055-94e2-478f-9768-bd28a6628bf5/AMSC_News_2012_12_5_Commercial.pdf

Contact: Jason Fredette, jason.fredette@amsc.com

►Wire 선 재료 線材料 [xiàn cáiliào]



Self-assembly Nanostructure in Superconductor

Oak Ridge National Laboratory (November 12, 2012)

Researchers at the Oak Ridge National Laboratory have made progress in the fabrication of advanced materials on a nanoscale. The spontaneous self-assembly of nanostructures composed of multiple elements is expected to lead to materials with an improved range of energy-efficient technologies and data storage devices. Specifically, the researchers are combining theoretical and experimental studies to understand and control the self-assembly of insulating barium zirconium oxide nanodots and nanorods within barium-copper-oxide superconducting films. Lead researcher on the project, Amit Goyal, summarized the research by stating, "We found that a strain field that develops around the embedded nanodots and nanorods is a key driving force in the self-assembly. By tuning the strain field, the nanodefects self-assembled within the superconducting film and included defects aligned in both vertical and horizontal directions." This method of controlled assembly greatly improved the material's properties, including a marked reduction in anisotropy. The findings have implications for the nanoscale fabrication of controlled self-assembled nanostructures comprised of multiple elements to be used in a range of electrical and electronic applications. The group's work was reported in *Advanced Functional Materials*.

Source: "'Strain tuning' reveals promise in nanoscale manufacturing"

Oak Ridge National Laboratory press release (November 12, 2012)

URL:

http://www.ornl.gov/info/press_releases/get_press_release.cfm?ReleaseNumber=mr20121112-01

http://www.eurekalert.org/pub_releases/2012-11/dml-tr111212.php

Contact: Bill Cabage cabagewh@ornl.gov

Superconductivity Web21

Published by International Superconductivity Technology Center
1-10-13, Shinonome, Koto-ku, Tokyo 135-0062, Japan Tel: +81-3-3536-7283, Fax: +81-3-3536-5717



Solution Deposition Planarization (SDP) System Installed Superconductor Technologies Inc. (November 12, 2012)

Superconductor Technologies Inc. (STI) has completed the acceptance testing of its Solution Deposition Planarization (SDP) system, which produces a wire template with a smooth surface—thereby eliminating the need to polish the template, which in turn reduced both costs and chemical waste. The equipment has now been shipped and received at STI's Advanced Manufacturing Center of Excellence in Austin, Texas. The milestone marks the completion of STI's new 2G HTS wire production suite at the Austin facility. The SDP system will be used in conjunction with an ion beam assisted deposition (IBAD) system that was installed last April to produce 1-km lengths of complete wire template. This template will then be used in a next-generation reactive co-evaporation cyclic deposition and reaction (RCE-CDR) system installed last October; the RCE-CDR equipment will deposit the HTS material onto the template using a proprietary process. The production line is expected to be completely installed and to be operational by the end of 2012, with commercial production anticipated in 2014.

Source: "Superconductor Technologies Inc. Completes Acceptance of Reactive Co-evaporation Cyclic Deposition and Reaction (RCE-CDR) Equipment for Its Conductus(R) 2G HTS Wire Production"

Superconductor Technologies Inc. press release (November 12, 2012)

URL:

[http://phx.corporate-ir.net/staging/phoenix.zhtml?c=70847&p=irol-newsArticle&ID=1757268&highlight=Superconductor Technologies Inc. Completes 2G HTS Wire Production Suite](http://phx.corporate-ir.net/staging/phoenix.zhtml?c=70847&p=irol-newsArticle&ID=1757268&highlight=Superconductor%20Technologies%20Inc.%20Completes%202G%20HTS%20Wire%20Production%20Suite)

Contact: Investor Relations, Cathy Mattison or Becky Herrick of LHA for Superconductor Technologies Inc., invest@suptech.com, ; HTS Wire, Mike Beaumont of STI, mbeaumont@suptech.com

► **Management and Finance** 경영정보 经营信息[jīngyíng xīnxi]



Financial Report

Superconductor Technologies Inc. (November 13, 2012)

Superconductor Technologies Inc. (STI) has reported its financial results for the third fiscal quarter ending September 28, 2012. STI's third quarter net revenues were US \$1.3 million, compared with \$479,000 for the same period in the previous fiscal year. The net loss for the third quarter was \$2.3 million, compared with \$3.3 million for the same period in the previous fiscal year. The company announced that it had reached a strategic milestone by completing the acceptance testing of all equipment required to produce Conductus® wire for commercial qualification. The production of longer lengths of wire for technical evaluation and qualification purposes is expected to begin in early 2013. Jeff Quiram, STI's president and chief executive officer, commented, "In the third quarter, our customer activities increased significantly, resulting in a full pipeline of requests for Conductus wire as customers seek to secure supply in 2013 and beyond. We expect the current demand associated with those requests will consume all the wire we can produce in the first few quarters of 2013."

Source: "Superconductor Technologies Reports Third Quarter 2012 Results"

Superconductivity Web21

Published by International Superconductivity Technology Center
1-10-13, Shinonome, Koto-ku, Tokyo 135-0062, Japan Tel: +81-3-3536-7283, Fax: +81-3-3536-5717

Superconductor Technologies Inc. press release (November 13, 2012)

URL: <http://phx.corporate-ir.net/staging/phoenix.zhtml?c=70847&p=irol-newsArticle&ID=1757840&highlight>

Contact: Investor Relations, Cathy Mattison or Becky Herrick of LHA for Superconductor Technologies Inc., invest@suptech.com, ; HTS Wire, Mike Beaumont of STI, mbeaumont@suptech.com



Cost Reduction Plan

AMSC (November 28, 2012)

AMSC has reduced its workforce by approximately 25 % and is consolidating office space so as to lower operating costs and enhance liquidity. The reductions have affected all of AMSC's major geographical locations and functions. The company's global workforce now consists of approximately 340 employees. Daniel P. McGahn, AMSC President and Chief Executive Officer, explained, "While the long-term prospects for renewable energy remain bright, conditions in the sector today are challenging. Financing and cash flow among wind farm developers and wind turbine manufacturers have been constrained, which has impacted growth plans for some of our Windtec™ Solutions partners. Given this environment, we made the difficult but prudent decision to reduce our workforce in order to weather the industry downturn and minimize our cash usage." The action is expected to reduce the company's annualized expenditures by approximately US \$10 million and should further lower its annualized operating expenses to less than \$58 million by the fiscal quarter ending June 30, 2013. Restructuring charges of \$3-\$4 million are anticipated during this period.

In response to shipment delays to Windtec Solutions partners, AMSC has also revised its financial forecast for the third fiscal quarter ending December 31, 2012. AMSC now expects revenues in excess of \$20 million and a net loss of less than \$24 million.

Source: "AMSC Announces Cost Reduction Action"

AMSC press release (November 28, 2012)

URL:

http://files.shareholder.com/downloads/AMSC/1729988020x0x617167/62572d2b-e268-442f-8808-783bbb19a9e2/AMSC_News_2012_11_28_Financial.pdf

Contact: Jason Fredette, jason.fredette@amsc.com

(Published in a Japanese version in the January 2013 issue of *Superconductivity Web 21*)

[Top of Superconductivity Web21](#)

Superconductivity Web21

Published by International Superconductivity Technology Center
1-10-13, Shinonome, Koto-ku, Tokyo 135-0062, Japan T el: +81-3-3536-7283, Fax: +81-3-3536-5717

Feature Article: SQUID Applications

- Utilizing HTS-SQUID for Non-destructive Testing Evaluating The Destructive Mechanism of Braided CFRPs

Yoshimi Hatsukade, Associate Professor
Department of Environmental & Life Sciences
Toyoashi University of Technology

The fabrication of lightweight airplanes and automobiles to attain energy savings and achieve improvements in fuel economies is currently being fulfilled using Carbon Fiber Reinforced Plastics (CFRPs). CFRPs are lightweight compared to general metals, offering superior specific strength and rigidity characteristics. Recent research and development efforts have sought braided CFRPs with greater strength and superior functionality. Developmental efforts in braiding bundles of carbon fibers have produced braided CFRPs (long and narrow textiles interwoven fibers oriented at an angle of 45°), with the continuously oriented fiber bundles of the composite structure able to support any load. This produces superior strength and elasticity characteristics over conventional CFRPs, and moreover an epoxy resin matrix coupled with a carbon nanofiller can be used to tailor its strength. Such techniques have produced a number of new braided fibrous assemblies all with differing characteristics.

With an HTS-SQUID gradiometer it is possible to detect breaks in carbon fiber bundles by visualization of current distribution. This was introduced in the August 2011 issue of Superconductivity Web21, where the possibility of assuming conductivity distribution within the materials was described. Following this, our joint research partner, Hamada research group based at Kyoto Institute of Technology, undertook tensile testing of the braided CFRPs and analyzed destructive process/material characteristics using both visual observations and stress-strain curves. Additionally, the group investigated the destructive mechanism of braided CFRPs by employing both destructive and non-destructive current distribution visualization testing methods, after unloading braided CFRPs during a destructive test.

For the test a 2 wt% carbon nanofiber (CNF), having an average diameter of 100 nm and about 10 μ m in length, were mixed into an epoxy resin matrix and combined with the flat-braided 25 carbon fiber bundles, producing braided CFRPs containing CNF. As a comparison, a reference braided CFRP without CNF has also been fabricated. The test observed the surface of the fiber and measured stress-strain curves with the application of a tensile load applied to the sample. The results from these tests are shown in upper half of Figure 1. Paint was applied to the sample surface after the application of a load to clearly identify surface cracking. A load applied to the reference braided CFRP without CNF, from an initial stage (1) showed a matrix crack down its left side, which reduced its stress (2), crack propagation then occurred along the matrix crack accompanied with an increase in strain, finally leading to breakage after several stress-strain cycles (3). On the other hand, the application of a load to the braided CFRP containing CNF, from an initial stage (1), produced several matrix cracks towards the lower side of the sample before finally cracking, but this time there

Superconductivity Web21

Published by International Superconductivity Technology Center
 1-10-13, Shinonome, Koto-ku, Tokyo 135-0062, Japan T el: +81-3-3536-7283, Fax: +81-3-3536-5717

was no accompanying decrease in stress (2), but was shortly followed by an abrupt crack emanating from one of those matrix cracks (3).

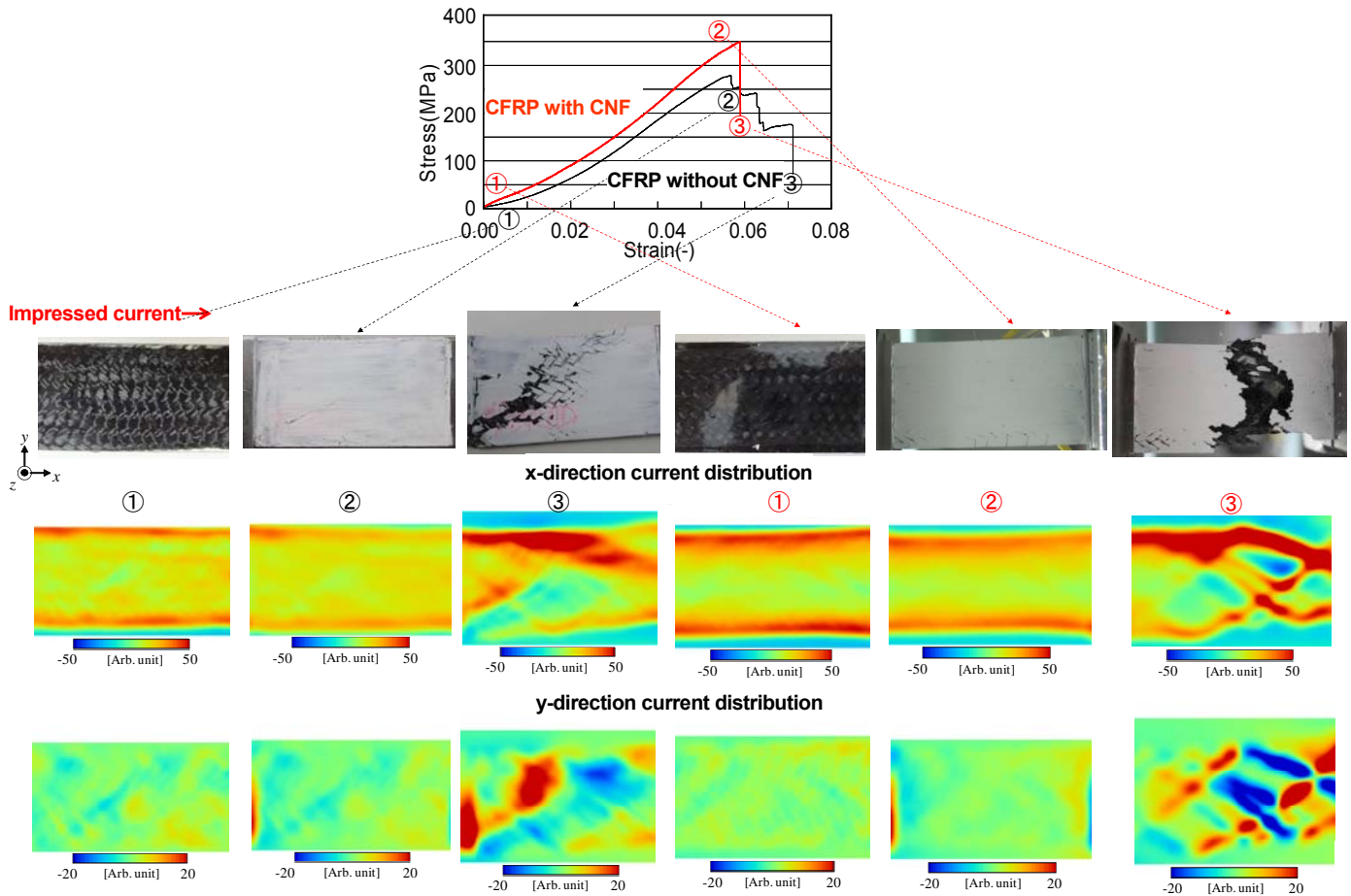


Fig. 1 (Top half) Stress-strain curves of braided CFRP with and without CNF, along with images after destruction. (Lower half) The visualization results of current distribution within braided CFRP by HTS-SQUID gradiometer. x-direction current distribution (mid-stage) and y-direction current distribution (lower stage) are shown separately.

The bottom half of Figure 1 shows current distribution visualization results, obtained using an HTS-SQUID gradiometer, when AC current was applied to the samples at each stage (1)-(3) as well as (1)-(3). Here, x-direction current distribution (mid-stage) and y-direction current distribution (lower stage) are shown separately. The upper figure shows the x-direction current flow, with deeper levels of red signifying greater current flow towards the right of the graph. Contrary to this, the lower figure shows the y-direction current distribution, with red and blue indicating current direction vertically. From the y-direction current distribution results, both samples indicate that the applied current travels 45° along braided carbon fiber bundles before a final crack occurs. Also, the current

Superconductivity Web21

Published by International Superconductivity Technology Center
1-10-13, Shinonome, Koto-ku, Tokyo 135-0062, Japan T el: +81-3-3536-7283, Fax: +81-3-3536-5717

distribution in the CNF-containing CFRP was far more homogeneous than the CFRP without CNF, and the edge effect across its width was greater. This effect was attributed to an average current density being measured around fiber bundles, since the current flows via CNF between fiber bundles, which are present amongst the carbon fiber bundles. As there was no observable difference in current distribution between the cracks occurring at (2) and (2), it was assumed that these were matrix cracks. However, there were large observable differences in current distribution due to fiber bundles breaking at the final crack stage of (3) and (3). The non-destructive test results shown in Figure 1 concluded that the braided CFRP without CNF underwent cracking in a majority of its fiber bundles, and also the CNF containing braided CFRP experienced a number of cracks within fiber bundles over its entire area. The CNF-containing CFRP underwent an abrupt final crack. It is believed that the CNF strengthened electrical conduction as well as mechanical load transmission between fiber bundles.

A combination of destructive and non-destructive testing were able to ascertain internal and external fiber information as well as correlate mechanical and electrical characteristics, thus indicating possible effectiveness of this technique as a potential destructive mechanism analysis method. Braided CFRP fibers in use today actually require methods to be able to detect initial crack formation, such as matrix cracks occurring between fiber bundles as observed in (2). Therefore, the development of eddy current detection technology has been currently progressing, a method that involves inducing current between fiber bundles to detect the formation of initial cracks. This series of research employs a multi-layered HTS SQUID gradiometer utilizing ramp-edge Josephson junction developed by ISTECS/SRL.

(Published in a Japanese version in the August 2012 issue of *Superconductivity Web 21*)

[Top of Superconductivity Web21](#)

Superconductivity Web21

Published by International Superconductivity Technology Center
1-10-13, Shinonome, Koto-ku, Tokyo 135-0062, Japan Tel: +81-3-3536-7283, Fax: +81-3-3536-5717

Feature Article: SQUID Applications

- Development of a Compact Magnetometer Using HTS-SQUID and a Rotating Sample

Kenji Sakai, Assistant Professor
Graduate School of Natural Science and Technology
Okayama University

1. Introduction

Magnetic susceptibility is a fundamental parameter specific to all magnetic materials. A non-destructive testing method involving measuring a material's magnetic susceptibility therefore allows material identification and the ability to evaluate the contents of specific materials. Although a magnetometer is typically employed for magnetic susceptibility measurement, the measurement method is different depending on the degree of magnetic susceptibility. A ferromagnetic material exhibits high magnetic susceptibility and has strong secondary magnetic fields generated with the application of an external magnetic field. For such cases a large-scale coil generating a strong magnetic field and a highly sensitive magnetic sensor are not required. On the other hand, paramagnetic and diamagnetic materials exhibit much lower levels of magnetic susceptibility and thus require the application of a strong magnetic field and employment of a highly sensitive magnetic sensor to detect weak magnetic fields generated by the materials. Presently the magnetic susceptibility of paramagnetic and diamagnetic materials is commonly undertaken by a magnetometer employing a high sensitive LTS-SQUID sensor. However, liquid helium cryocooling is required in addition to issues with system footprint, difficulties in maintenance and management concerns related to high running costs. Current commercially available magnetometers that utilize LTS-SQUIDs occupy large areas of laboratory space and installation space has to be determined prior to the installation. Additionally, there are also limitations placed on quantity and shape of samples that the system can handle and are mostly limited to solid matter or powders. Liquid samples are difficult to handle, with only a handful of studies reporting liquid magnetic susceptibilities measured with a high degree of sensitivity. To address these issues our research group has been tasked with the development of a compact, desktop-sized magnetometer that employs an HTS-SQUID, which has far easier cryocooling requirements and lower running costs. The HTS-SQUID employed in this study was a ramp-edge Josephson Junction developed at ISTEC/SRL.

2. The system design and the measurements results

A schematic of the system developed is shown in Figure 1. The sample is fixed to a disc rotated by an ultrasonic motor, and transferred between the poles of an electromagnet. The magnetic field emanating from a sample is detected as follows. The electromagnet generates a DC magnetic field that magnetizes the sample as it passes between the poles. As shown in Figure 1, a first order differential pick-up coil is installed below the poles and detects changes in magnetic field as the rotating sample passes by. The detected signal is fed to the HTS-SQUID via an input coil connected in series to the pick-up coil. Here, the SQUID and input coil are magnetically shielded, thereby allowing samples to be easily replaced/fitted. Although a sample holder with dimensions of 25x25x19mm² has been employed for the purposes of this demonstration, the system can house different shapes and sizes of sample holder, to a certain degree. Additionally, the sample holder can accommodate liquid samples thereby offering advantageous characteristics and greater flexibility in measuring liquids sample.

Superconductivity Web21

Published by International Superconductivity Technology Center
1-10-13, Shinonome, Koto-ku, Tokyo 135-0062, Japan T el: +81-3-3536-7283, Fax: +81-3-3536-5717

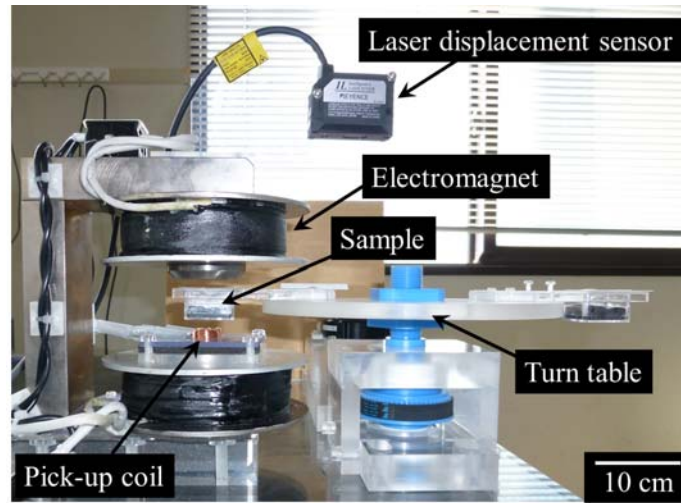


Fig. 1 A compact magnetometer

Evaluation of the system has been performed using a composite consisting of resin and ferromagnetic iron oxide particles, and pure water - a diamagnetic liquid. Figure 2 shows the output SQUID waveform from each sample. Collecting data from many samples rotations reduced data noise and a laser displacement sensor determined specific sample locations, allowing computation of arithmetic mean. The ferromagnetic sample produced a particular waveform as shown in Figure 2(a), which was attributed to the first order differential coil, and also produced an output voltage that was larger compared to that of pure water. On the other hand, although the output voltage from pure water was small, the particular waveform attributed to the first order differential coil was similar to Figure 2(a). This confirmed the systems ability to detect a weak magnetic fields generated by pure water. Furthermore, comparing Figures 2(a) and (b) reveals a 180° phase change between the waveform patterns of the ferromagnetic material and pure water. This indicates that because of the diamagnetic material of pure water the secondary magnetic fields generated by the application of an external magnetic field are opposite to that of ferromagnetic materials. Thus, the findings of this study clarified that the magnetic fields measured by the system were able to identify ferromagnetic/paramagnetic and diamagnetic materials.

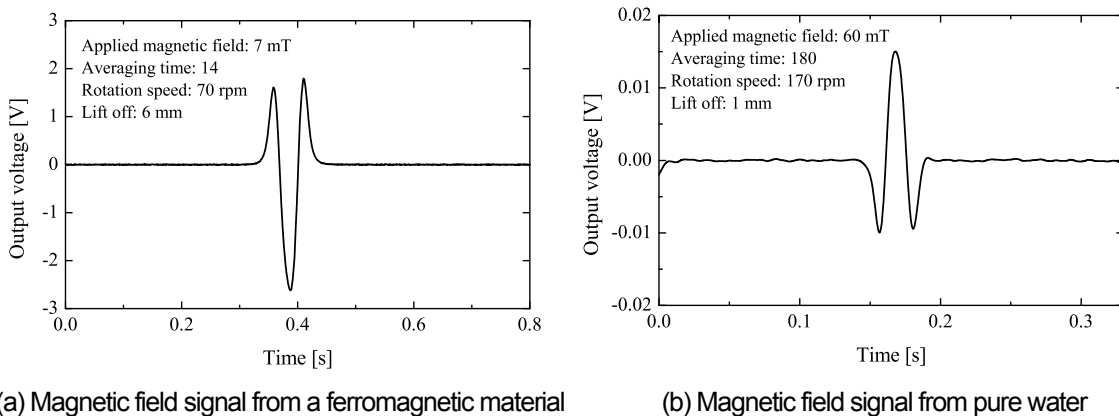


Fig. 2 (a) Magnetic field signal from a ferromagnetic material and (b) magnetic field signal from pure water, as measured using the magnetometer developed in this work

Superconductivity Web21

Published by International Superconductivity Technology Center
1-10-13, Shinonome, Koto-ku, Tokyo 135-0062, Japan T el: +81-3-3536-7283, Fax: +81-3-3536-5717

3. Conclusions

We have developed a highly sensitive magnetometer that is very compact and allows measurements to be made easily. Measurements detecting weak magnetic fields generated from pure water were successful. The system will be further improved in the future to include a plan to investigate new measuring system able to determine moisture content and perform identification/quantitative evaluation of materials.

The research findings were supported by the Strategic Promotion of Industry-Academia Innovative R&D, JST.

(Published in a Japanese version in the August 2012 issue of *Superconductivity Web 21*)

[Top of Superconductivity Web21](#)

Superconductivity Web21

Published by International Superconductivity Technology Center
1-10-13, Shinonome, Koto-ku, Tokyo 135-0062, Japan T el: +81-3-3536-7283, Fax: +81-3-3536-5717

Feature Article: SQUID Applications - Development of A Biological Immunoassays Employing Magnetic Markers (HTS-SQUID)

Kenji Enpuku, Professor
Research Institute of Superconductor Science and Systems
Kyushu University

Magnetic markers are nanometer-sized polymer-coated magnetic particles that are immobilized with test reagents on their surfaces. Such markers are routinely employed in several types of medical and biological applications. Representative applications include separation/purification of proteins and cells, MRI contrast media, magnetic hyperthermia and magnetic immunoassays. Amongst those applications biological immunoassay is often applied in medical diagnosis to detect disease-causing proteins and pathogenic bacteria.

Magnetic-based immunoassay detects binding reactions between magnetic markers and biological targets by measuring magnetic signals from the markers. This method is expected to offer greater new functionalities over conventional optical-based markers. A couple of benefits afforded by magnetic markers over optical markers are, 1) the possibility to undertake a liquid phase immunoassay without the need of a bound/free (B/F) separation, usually difficult with the optical method, leading to more swift and greater detection sensitivity, and 2) it could evolve as an internal medical diagnosis method able to measure binding reactions in the body since the magnetic signal permeates through the body.

Here, the detection of small concentrations of biomaterials is dependent upon the ability to detect micro magnetic fields emanating from magnetic markers. Also, employing a SQUID sensor then offers the potential of a highly sensitive detection system. This article introduces our research pertaining to bio immunoassay taking advantage of the characteristics afforded by the above-mentioned magnetic marker technology.

Firstly, liquid phase immunoassay is introduced. It's aimed at external medical diagnosis applications such as blood testing. As shown in Figure 1(a), an antigen is immobilized on a polymer particle, 3.3 μm in diameter, to which the target is combined. After combining, the magnetic markers are fed to the liquid; some combine and form bound markers whilst others remain free. The different magnetic characteristics between the markers allow them to be magnetically distinguished without using the "washing process".

Figure 1(b) is an example of a protein called biotin that has been detected using this method. The abscissa shows the numbers of biotin N_B , and the ordinate shows the magnetic signal detected by the SQUID. It was possible to detect up to 10^5 biotins. The detection sensitivity was 6 atto-mol/ml, confirming that micro detection to atto-mol levels was possible. The sensitivity was compared utilizing MR (magnetic resistance) and FG (flux gate) sensors, and clearly showed that a SQUID allows the detection micro-amounts of biotins.

The development of an immunoassay involving internal medical diagnosis is now introduced. An example of internal diagnosis employing a magnetic marker is displayed in Figure 2(a), which shows a sentinel lymph node biopsy carried out on a breast cancer cell. Magnetic markers injected into diseased tissues

Superconductivity Web21

Published by International Superconductivity Technology Center
 1-10-13, Shinonome, Koto-ku, Tokyo 135-0062, Japan T el: +81-3-3536-7283, Fax: +81-3-3536-5717

(cancel cells) reach the first lymph node (sentinel lymph node) via the lymph duct. If a cancer cell spreads to this lymph node then the magnetic marker binds with the cancer cell and is accumulated at that point. Thus, body-surface-measurements of magnetic signals generated from magnetic markers concentrated in the lymph node allow possible detection and thus provide an early sign of potential cancer cells spreading. This method of detecting the quantity and the location of magnetic markers concentrated inside a body is generally referred to as Magnetic Particle Imaging (MPI).

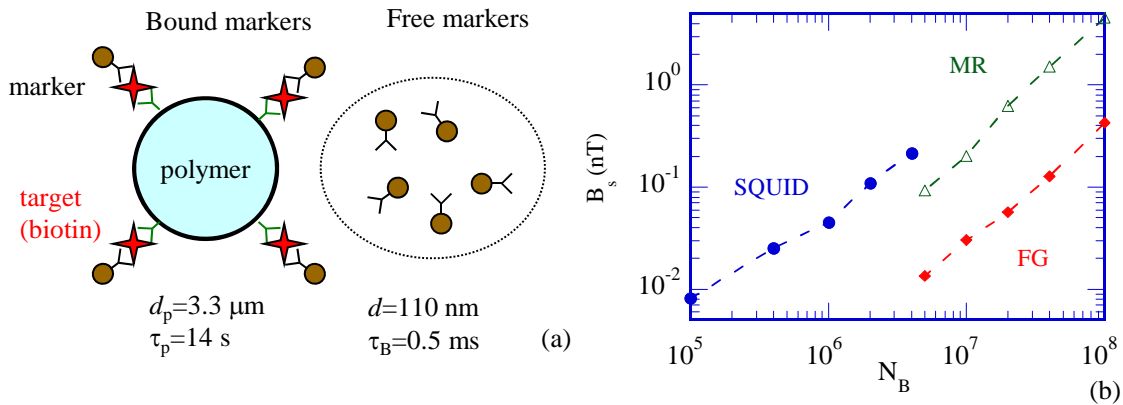


Fig. 1 (a) Magnetic markers in liquid phase immunoassay,
 (b) Detection of biotin – the relationship between the numbers of biotin N_B and magnetic signal strength

Figure 2(a) shows magnetic marker image simulations of two markers (each 5 mmφ in size, 100 μg in weight), both deeply located $z=20$ mm and separated from each other by a distance $\Delta x=20$ mm, with the resultant signal field map at the location $z=0$ mm (corresponding to the body surface) in Figure 2(b). In the same figure, the presence of these two magnetic markers is apparent from the peak in the vertically generated magnetic field from the markers. However, since the field map is spatially spreading as shown in Figure 2(b), the spatial resolution of the map estimating the location of the markers decreases. Figure 2(c) shows the magnetic marker distribution results obtained from a field map calculated using a singular value decomposition (SVD) method. This technique clearly distinguishes the location of the two markers. Thus, it becomes possible to precisely detect the location and quantity of magnetic markers accumulated within a body and paves the way for the future development of immunoassay deployed for internal medical diagnosis.

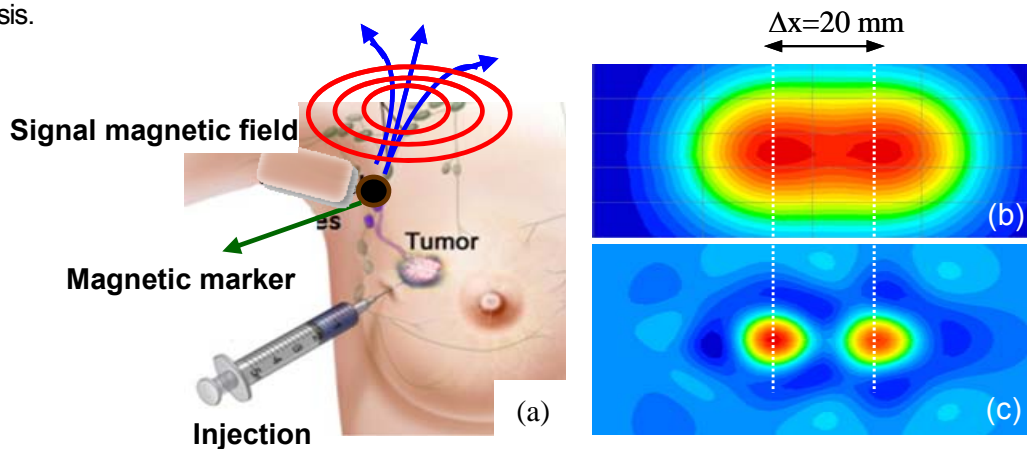


Fig. 2 (a) Magnetic marker imaging for internal medical diagnosis, (b) Field map from two magnetic markers,
 (c) Estimating the location of two magnetic markers

Superconductivity Web21

Published by International Superconductivity Technology Center
1-10-13, Shinonome, Koto-ku, Tokyo 135-0062, Japan T el: +81-3-3536-7283, Fax: +81-3-3536-5717

This research has been jointly undertaken with Nagasaki International University and Central Research Laboratory, Hitachi, Ltd.

(Published in a Japanese version in the August 2012 issue of *Superconductivity Web 21*)

[Top of Superconductivity Web21](#)

Superconductivity Web21

Published by International Superconductivity Technology Center
1-10-13, Shinonome, Koto-ku, Tokyo 135-0062, Japan T el: +81-3-3536-7283, Fax: +81-3-3536-5717

Feature Article: SQUID Applications

- A Large-scale Magnetic Field Gradiometer Utilizing YBCO High Temperature Superconducting Tapes

Akira Tsukamoto
Senior Research Scientist
Electronic Devices Division
SRL/ISTEC

A transient electromagnetic method (TEM) employing a high temperature superconducting SQUID has been developed both in Japan and overseas for mining exploration, commencing now with a practical device for metals exploration. The method involves the transmission of a pulse current of several tens of amperes travelling in a 100-200m long (length of one side) loop coil laid on the ground, and determining underground resistivity features by monitoring attenuation characteristics of a secondary magnetic field generated from induced current dispersion underground. The high sensitivity characteristics afforded by a SQUID allows for greater exploration depths compared to a conventional TEM method employing an induction coil as a sensor. However, increased SQUID sensitivity leads to an increased influence of environmental magnetic noise. In order to address this a gradiometer measuring a magnetic field gradient between two points has been used to cancel environmental noise, leading to an expectation that measurements of magnetic field gradient can further improve sensitivity at boarder regions. Nevertheless, a long baseline (the distance between two points to be measured) was required in order to measure a magnetic signal from underground in several tens or several hundred meters depth.

Until now, it is difficult to fabricate a large-scale gradiometer due to the lack of technological development in joining the high temperature superconducting wires in a superconducting state. The Superconductivity Research Laboratory has however been successful in developing a large-scale magnetic field gradiometer that allowed YBCO tapes and high temperature SQUID devices to be connected with a low contact resistance.

Figure 1 shows a schematic and a photo of the large-scale magnetic field gradiometer developed in this study. The pickup coil was fabricated utilizing a 10 mm-wide Gd123-based high temperature superconducting tape (made by Fujikura). The tape was divided into two 5 mm-width pieces with both terminal ends connected, was wound three-dimensionally into a bobbin having a 100mm diameter. This realized a planar type first-order gradiometric pickup coil without bonding (Figure 1). Employing long tapes allows coils to be fabricated with specific winding turns. The SQUID device utilized here forms a directly-coupled thin film gradiometer in which the SQUID device accommodates the first-order thin film pickup coil connected directly to the inductor. The input coil connecting the thin film pickup coil was fabricated on a substrate different to that of the SQUID device and the directly coupled thin film gradiometer was attached by an epoxy adhesive to the top of the input coil, forming a flip-chip style structure. The magnetic field gradiometer has 26 turns on the input coil (N_i) and 6 turns on the pickup coil (N_p), allowing reliable inductance matching. A low melting point alloy (melting point 79°C) was used to connect the input coil with the pickup coil. In addition to increased detection sensitivity it is also important for the gradiometer to keep a balance between the two pickup coils. We have developed a balance adjusting mechanism that attaches three YBCO tapes to an eccentric rotating plate. Depending upon the point of rotation the relative

Superconductivity Web21

Published by International Superconductivity Technology Center
 1-10-13, Shinonome, Koto-ku, Tokyo 135-0062, Japan T el: +81-3-3536-7283, Fax: +81-3-3536-5717

inner and outer positions of the YBCO tapes connecting the detection coil vary continuously, allowing magnetic flux linking the pickup coils to be adjusted.

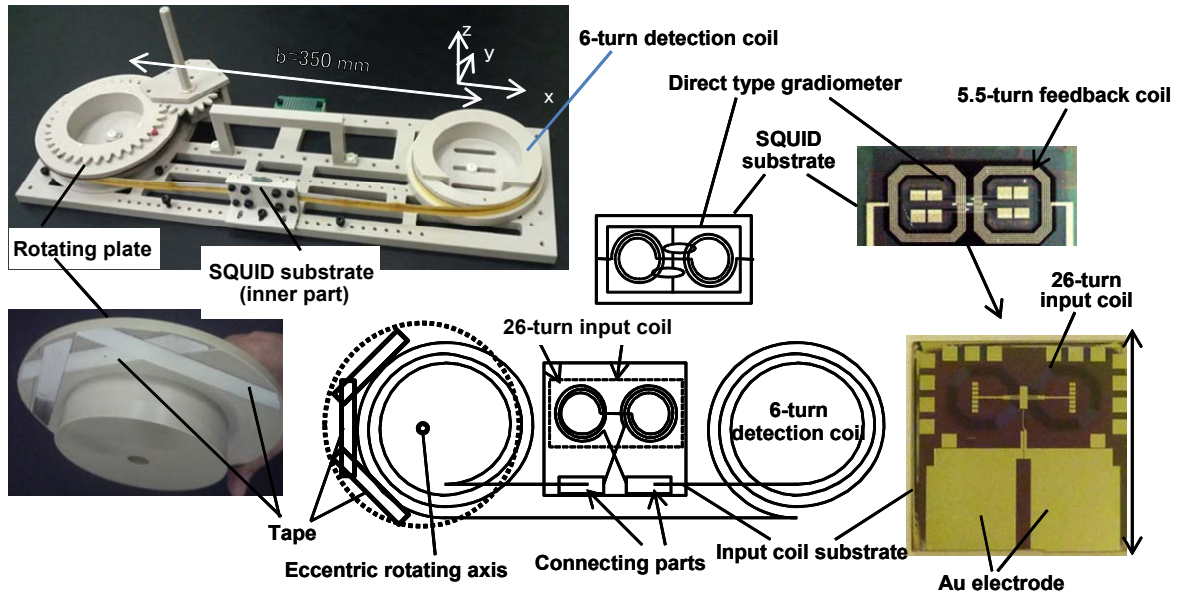


Fig. 1 A schematic of the large-scale magnetic field gradiometer developed

Figure 2 shows the measured frequency characteristics of the magnetic field gradiometer ($N_i=26, N_p=6$). The sensitivity characteristics were flat at greater than 9Hz of the cut-off frequency. A deterioration of sensitivity at lower frequencies was due to the influence of contact resistance. Sensitivity at flat region corresponding to an effective area of 1.89 mm^2 and an effective volume of 662 mm^3 , defined as effective area \times baseline. The magnetic flux noise was as low as $25 \mu\Phi_0/\text{Hz}^{1/2}$ (white), which corresponding to gradient magnetic field noise of around $1 \text{ fT}/\text{cm} \cdot \text{Hz}^{1/2}$ (white). Gradiometer balance was 1/142 (1/69 recorded before balance adjustments). Mining exploration requires a balance performance of about 1/1000 therefore further precise balance adjustments are considered necessary.

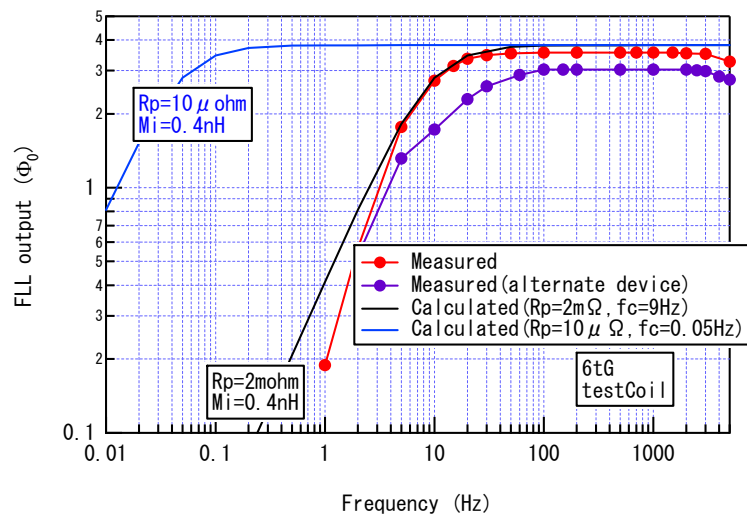


Fig. 2 Frequency characteristics of the magnetic field gradiometer
 (A comparison between actual and calculated values)

Superconductivity Web21

Published by International Superconductivity Technology Center
1-10-13, Shinonome, Koto-ku, Tokyo 135-0062, Japan T el: +81-3-3536-7283, Fax: +81-3-3536-5717

This research was commissioned by Japan Oil, Gas and Metals National Corporation (JOGMEC), as a part of a mineral exploration, project funded by the Ministry of Economy, Trade and Industry.

(Published in a Japanese version in the August 2012 issue of *Superconductivity Web 21*)

[Top of Superconductivity Web21](#)

Superconductivity Web21

Published by International Superconductivity Technology Center
1-10-13, Shinonome, Koto-ku, Tokyo 135-0062, Japan T el: +81-3-3536-7283, Fax: +81-3-3536-5717

Feature Article: SQUID Applications

- Realizing A SQUID Magnetometer for Practical Geomagnetic Field Measurements

Jun Kawai, Professor
Applied Electronics Laboratory
Kanazawa Institute of Technology

1. Introduction

Observations of terrestrial electromagnetic phenomena including geomagnetic field have long since been performed in order to study earth's dynamism, as well as investigating physics-related phenomena such as auroras and geomagnetic storms occurring at the magnetosphere. Research in this field has recently progressed whereby electromagnetic phenomena emanating from crustal movements such as earthquakes and volcanic activities can be detected (Hayakawa 2010). There were recent reports of an extraordinary increase in the outgoing long wave radiation (OLR) close to the epicenter prior to and after the M9.0 earthquake that struck the east coast of Japan in 2011 (Ouzounov 2012). It is the author's belief that changes in the ionosphere due to crustal movements could be detected by measuring minute ground surface changes in geomagnetic field. In fact, there was a recent report from an overseas research facility utilizing an abandoned mine (France: LSBB), who were able to detect minute magnetic signals of around 100pT~1nT by employing a SQUID, assuming that the ionosphere was excited by crustal movements (Waystand 2009).

Conventionally, either a fluxgate magnetometer or an overhauser magnetometer has been utilized for detecting changes in geomagnetic field. Greater sensitivity for geomagnetic field measurements using more highly sensitive SQUIDs have been proposed earlier with experiments undertaken in Japan (Kitamura 1978, Kamata 2000). Additionally, field measurement trials close to volcanic areas have also been performed using a portable HTS-SQUID device (Kasai 2001, Nomura 2002, Machitani 2003). Despite this, it is difficult to ascertain whether a stable SQUID system applicable for the long-term continuous measurements of geomagnetic field has been established. Thus, in order to address this, the author's research team has performed long-term field experiments to verify the potential practicability of a SQUID system for field measurements. The study has been to determine whether a practical SQUID system is feasible, and prove *"the effectiveness of a SQUID as a highly-sensitive tool for measuring changes in geomagnetic field, even though the inconvenience of requiring liquid helium coolants and the inability to measure absolute values are unavoidable."*

2. The prototype system and field measurements

The system fabricated at this time consisted of a SQUID magnetometer, designed to detect the XYZ components of geomagnetic field, a cryostat, a direct read-out FLL system, an amplifier circuit and both an analog low and high-pass filter. The schematic on the left of Figure 1 shows an outline picture of a 3-axis SQUID magnetometer. The Nb-based SQUID magnetometer, having dimensions of 2.5 mm x 2.5 mm, is a flux-transformer type. The middle picture of Figure 1 shows the cryostat made of GFRP, 0.42 m diameter and 1m tall, with a 35-L liquid helium capacity, allowing a month-of continuous cooling. The system noise, as evaluated by a SQUID installed within the superconducting shield was measured as $15 \text{ fT}/\sqrt{\text{Hz}}$ and 2

Superconductivity Web21

Published by International Superconductivity Technology Center
1-10-13, Shinonome, Koto-ku, Tokyo 135-0062, Japan T el: +81-3-3536-7283, Fax: +81-3-3536-5717

$\text{pT}/\sqrt{\text{Hz}}$ at 100 Hz and 0.01 Hz, respectively. The low frequency noise, which is attributed to the temperature drift in the output of the preamplifier, was measured to be $6.5 \text{ pT}/^\circ\text{C}$ on a magnetic field conversion basis. This is an issue to be addressed in the future. The DC-offset generated during SQUID FLL operation is canceled with the additional field applied through the feedback coil in the SQUID. An electromagnetic shield placed around the SQUID magnetometer eliminated high frequency noise and limited the overall frequency bandwidth to around DC~500 Hz. By taking into consideration the diurnal variation of geomagnetic field, the maximum detectable field was set at $\pm 150 \text{ nT}$. Using a commercially available 16-bit data logger has been employed for data collection, the minimum measurable magnetic field has been presently limited to 15 pT due to guaranteed resolution. If required, increased data logging resolution up to the noise level of the SQUID is conceivable. Furthermore, a GPS pulse signal allows data time correction.

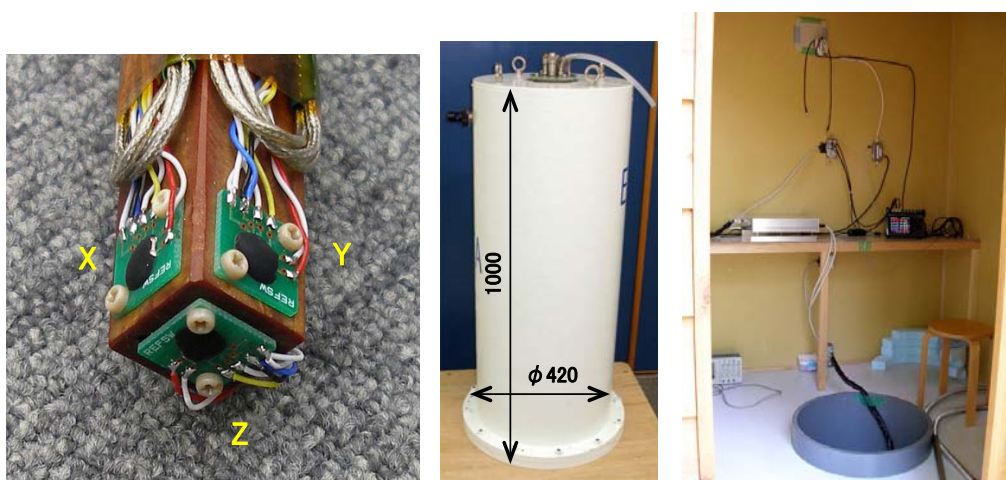


Fig. 1 (left) 3-axis SQUID magnetometer , (middle) Cryostat, (right) Inside experiment facility

A wooden building was constructed on the ground floor of our laboratory for the experimental field measurements. The system was installed in April last year and since then has been continuously making measurements in order to ascertain its practicability. The picture on the right hand side of Figure 1 shows inside the facility. The geographical coordinates of the facility are $36^\circ 30'00.8''$ north and $13^\circ 41'51.5''$ east, and is located 199m above sea level. The cryostat is housed in a hole constructed on the ground floor with the SQUID sensors buried 1m below the ground. Also, a 3-axis accelerometer has been installed on top of a granite pillar buried in the ground floor to measure vibration. For measurements to generally determine changes in geomagnetic field, the specifications of the system allow it to measure very low frequencies of several seconds to frequencies of several 1000s of seconds. Thus, it is imperative that changes in DC are precisely measured without any anomalies due to errors such as flux jumps. Ongoing studies are currently underway with measurements taken every few days by the authors' team.

The left hand side of Figure 2 shows an example signal of the changes in geomagnetic field measured with this system over two days, from 12-14th May 2012. The frequency bandwidth was set at DC~20 Hz and the sampling frequency was 50 Hz. The X, Y, Z axis correspond to north-south, east-west and vertical, respectively. Although the experimental period was short, the changes in the geomagnetic field are successfully measured. The right hand image of Figure 2 shows the data obtained for a period of 1 hour from 22:00, 12 May (JST), south-north element (B_x) after high-pass filtering with a 150-second cut-off. This finding confirms that a geomagnetic pulsation, called Pi2, was successfully detected.

Superconductivity Web21

Published by International Superconductivity Technology Center
1-10-13, Shinonome, Koto-ku, Tokyo 135-0062, Japan T el: +81-3-3536-7283, Fax: +81-3-3536-5717

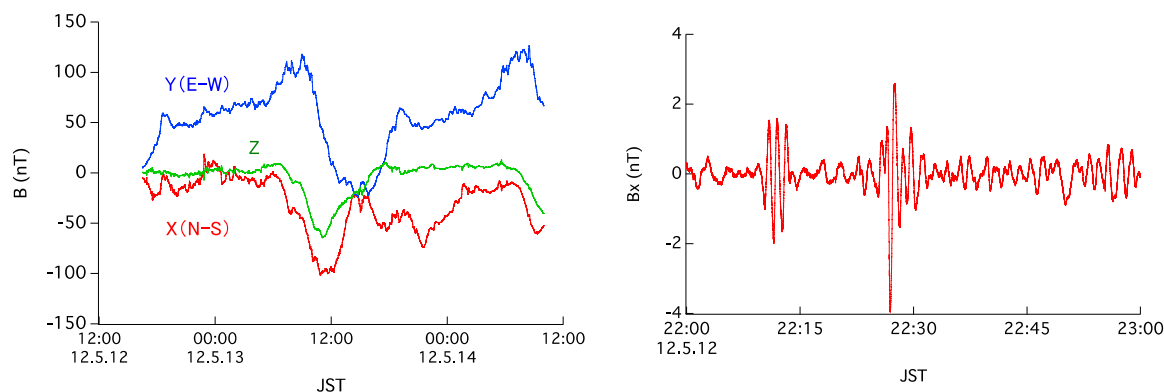


Fig. 2 (left) The changes in geomagnetic field measured by SQUIDs,
(right) Pi2 geomagnetic pulsation detected by SQUID

3. Conclusions and future issues

A highly sensitive system employing a SQUID to measure changes in geomagnetic field has been developed and field experiments have been demonstrated. Further detailed evaluation of this system due to climate and environmental noise and analysis of the obtained data are planned. Whilst experiments addressing issues of “*what is required to optimize SQUID system designed for field measurements of geomagnetic field*” are ongoing, enhancements in the system performance are currently continuing for the realization of a practical system.

(Published in a Japanese version in the August 2012 issue of *Superconductivity Web 21*)

[Top of Superconductivity Web21](#)

Superconductivity Web21

Published by International Superconductivity Technology Center
1-10-13, Shinonome, Koto-ku, Tokyo 135-0062, Japan T el: +81-3-3536-7283, Fax: +81-3-3536-5717

Feature Article: SQUID Applications

- Ultra-low-Field NMR Measurements of Protons and Fluorine Nuclei using SQUID

Yusuke Seki
Central Research Laboratory
Hitachi, Ltd.

1. Introduction

Recent years have seen attention focused on employing a superconducting quantum interference device (SQUID) in NMR/MRI measurements performed in the so-called ultra-low field 10–100 microtesla (μT) range, and offering equivalent static magnetic field strength characteristics as those observed at the terrestrial magnetic level^{1,2}. The static magnetic field strength of conventional NMR/MRI is a few tesla and signal frequency (proton magnetic resonance frequency) is around 100 MHz. However, ultra-low-field NMR/MRI has a static magnetic field strength of around 10–100 μT and a signal frequency of around 1–10 kHz, 5–6 orders of magnitude lower than conventional NMR/MRI. Ultra-low field NMR/MRI detects NMR signals by employing a highly sensitive SQUID-based magnetic sensor coupled with a technique to increase sample signal strength by pre-polarization of the nuclear spins at around 10–100 mT.

A copper wire coil makes up both the ultra-low field static magnetic and gradient field coils at room temperature, offering the potential of realizing a compact, low cost and much safer alternative compared to a superconducting magnet. Also, since the signal frequency is low in the kHz order it potentially enables NMR/MRI measurements to be undertaken even for metal contamination measurements³. Additionally, simultaneous magnetoencephalography measurements are made feasible, which were impossible with conventional MRI⁴. Furthermore, there are additional indications that the longitudinal relaxation time (T_1) image contrast has the potential to detect tissues/materials such as tumors and flammable liquids, which have until now been difficult to detect using high field MRI^{5,6}. Employing a SQUID is far superior in terms of broadband measurements when compared to detection methods employing induction coils, which require a resonance circuit.

The author and his group have been advancing their research in ultra-low-field NMR/MRI studies aiming for the development of new biometric technology. This article provides a brief account of the research undertaken in the simultaneous measurements of ultra-low-field NMR signals emanating from protons and fluorine nuclei, which have different resonant frequencies, and focuses on the characteristics of employing a SQUID detection method that offers far superior broadband characteristics as mentioned above.

2. System configuration of ultra-low-field NMR

Figure 1 shows a schematic of the prototype ultra-low-field NMR fabricated for this research. The hardware comprises a SQUID gradiometer for signal detection and a coil system designed to generate a magnetic field to test the samples. For this research an axial second-order gradiometer employing low- T_c SQUID (50 mm in diameter, 70 mm in baseline, $0.65 \text{ fT/Hz}^{1/2}$ magnetic field noise) was fabricated.

Superconductivity Web21

Published by International Superconductivity Technology Center
1-10-13, Shinonome, Koto-ku, Tokyo 135-0062, Japan T el: +81-3-3536-7283, Fax: +81-3-3536-5717

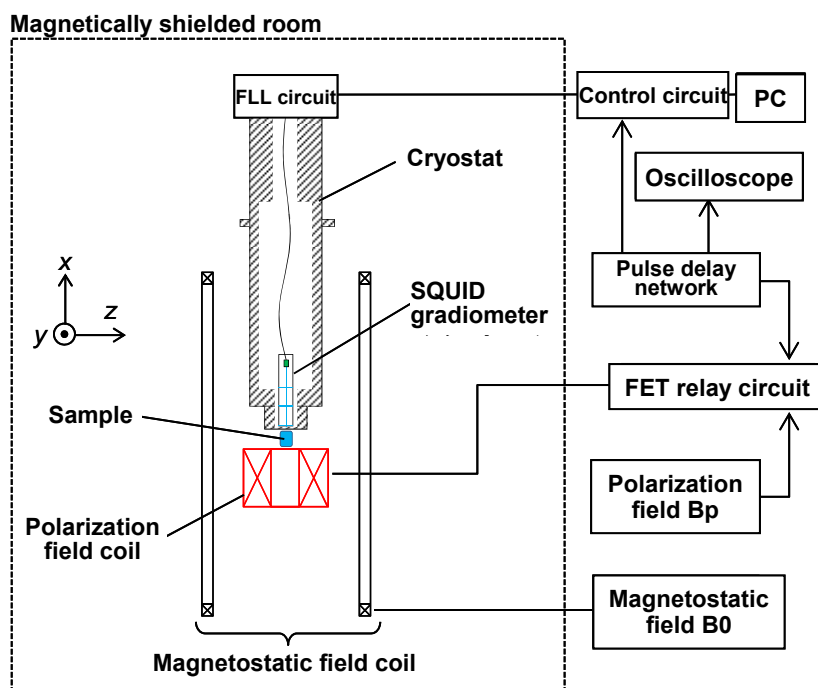


Fig. 1 Schematic of the ultra-low-field NMR

A polarizing magnetic field coil is used to magnetize the sample and plays an important role in increasing signal strength. It is also desirable that the current passing through the polarizing magnetic field coil can be switched off rapidly. From this perspective, the polarizing magnetic field coil was fabricated by winding low impedance, high-frequency Litz wire (72 strands) having 1550 turns filling a bobbin (110 mm in diameter, 178 mm in length). A FET relay switching circuit was employed to rapidly switch off the current passing through the polarizing magnetic field coil.

The static magnetic field coil was arranged in a Helmholtz pair configuration with two coils placed parallel to each other. It is necessary that the radius of the Helmholtz coil be equal to or greater than the separation distance between the coils in order to have a homogeneous magnetic field around a central area where the sample is located. For this study the Helmholtz coils had a diameter of 1.2 m and were separated by 0.53 m. The direction of the static magnetic field B_0 (z-direction) was vertical to the direction of the polarization magnetic field B_p (x-direction), and a static magnetic field intensity was $50 \mu\text{T}$, equivalent to an earth's magnetic field.

3. NMR measurements

Figure 2 shows the imaging sequence measured by the NMR employed in this research. The polarization magnetic field B_p magnetizes the nuclear spin within a sample in the x-direction. When the current passing through the polarization field is switched off the nuclear spin is magnetized in the direction of the static magnetic field B_0 . At this time, the NMR signal generated from within the sample has a resonance frequency equal to $f_0 = \gamma B_0 / 2\pi$ in the direction of the polarized field and is attenuated at a transverse relaxation time of T_2 . The gyromagnetic ratio γ is a constant and it is well known to have specific values for each individual nuclei. This is most basic NMR signal and is called the free induction decay (FID).

Superconductivity Web21

Published by International Superconductivity Technology Center
1-10-13, Shinonome, Koto-ku, Tokyo 135-0062, Japan T el: +81-3-3536-7283, Fax: +81-3-3536-5717

For this study the polarization magnetic field B_p and static magnetic field B_0 were set as 17 mT and 50 μ T, respectively. The static magnetic strength was measured using a fluxgate magnetometer. The application duration time of the polarized magnetic field was 5 s, with the measurement using the SQUID gradiometer, starting 20 ms after the polarized field was switched off. Data was acquired using an oscilloscope for a period of 250 ms after the polarized magnetic field was switched off and at a sampling rate of 10 kHz after passing through 1.6–2.5 kHz band-pass filter. Furthermore, the NMR signal spectra were FFT processed from the waveform obtained.

Samples for NMR measurements involved 15 ml of pure water (H_2O) and 15 ml of fluorine compound perfluorooctane (C_8F_{18}), which has an extremely low concentration in the human body and is widely used as MRI contrast media.

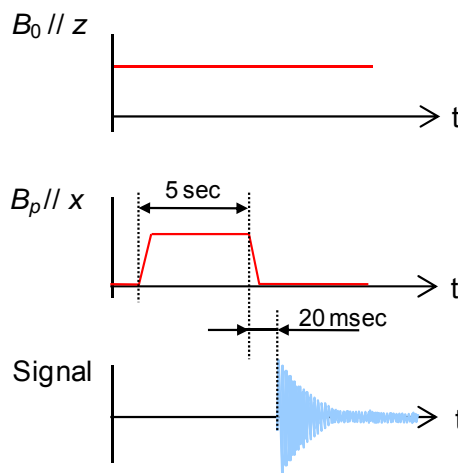


Fig. 2 NMR Measurement Sequence

Figures 3(a) and 3(b) show the FID signals obtained from the samples and the NMR spectra acquired after FFT processing, respectively. The data acquisition shown in Fig. 2 is from a one-time sequence, obtained without determining the arithmetic mean. The results clearly show that protons have a peak resonance frequency of 2158 Hz, whereas fluorine nuclei have a peak resonance frequency at 2031 Hz, and both corresponding to a static magnetic strength of 50.7 μ T. The signal-to-noise ratio was about 10. Moreover, the FID signal shown in Fig. 3(a) confirmed a beat signal corresponding to the difference of 127 Hz between the resonance frequencies of protons and fluorine nuclei.

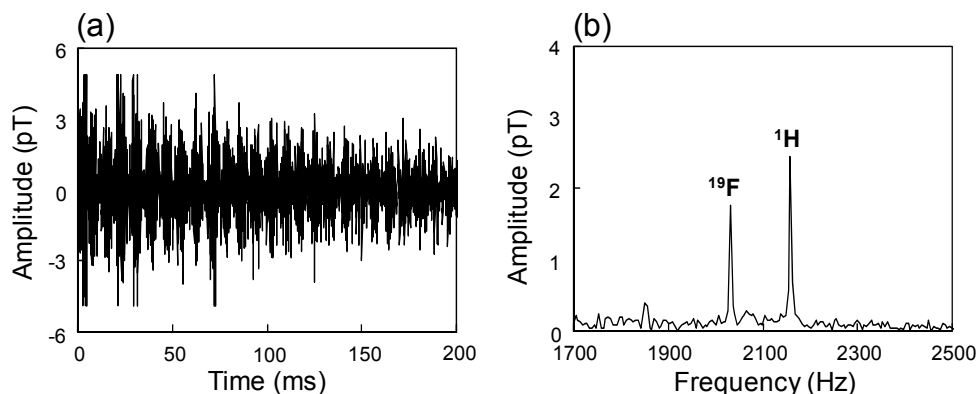


Fig. 3 (a) FID signals and (b) NMR spectra of pure water and perfluorooctane.

Superconductivity Web21

Published by International Superconductivity Technology Center
1-10-13, Shinonome, Koto-ku, Tokyo 135-0062, Japan T el: +81-3-3536-7283, Fax: +81-3-3536-5717

4. Conclusions

NMR measurements have been performed using pure water and perfluorooctane samples at static magnetic strength of 50 μ T to validate the performance attributes of an ultra-low-field NMR system employing a SQUID. The results showed the simultaneous detection of both protons and fluorine nuclei with different resonance frequencies, obtained without an arithmetic mean. Therefore the experiments verified the highly sensitive performance attributes of a prototype ultra-low-field NMR system able to simultaneously measure the magnetic resonant signal derived from several atomic nuclei.

References:

1. R. McDermott, S-K. Lee, B. Ten Haken, A. H. Trabesinger, A. Pines, and J. Clarke, *Proceedings of the National Academy of Sciences* 101, 7857–62 (2004).
2. J. Clarke, M. Hatridge, and M. Mößle, *Annual Review of Biomedical Engineering* 9, 389–413 (2007).
3. M. Mößle, S. I. Han, W. R. Myers, S. K. Lee, N. Kelso, M. Hatridge, A. Pines, and J. Clarke, *Journal of Magnetic Resonance* 179, 146–151 (2006).
4. V. S. Zotev, A. N. Matlashov, P. L. Volegov, I. M. Savukov, M. A. Espy, J. C. Mosher, J. J. Gomez, and R. H. Kraus, Jr., *Journal of Magnetic Resonance* 194, 115–120 (2008).
5. S. Busch, M. Hatridge, M. Mößle, W. Myers, T. Wong, M. Mück, K. Chew, K. Kuchinsky, J. Simko, and J. Clarke, *Magnetic Resonance in Medicine* 67, 1138–1145 (2012).
6. M. Espy, M. Flynn, J. Gomez, C. Hanson, R. Kraus, P. Magnelind, K. Maskaly, A. Matlashov, S. Newman, T. Owens, M. Peters, H. Sandin, I. Savukov, L. Schultz, A. Urbaitis, P. Volegov, and V. Zotev, *Superconductor Science and Technology* 23, 034023 (2010).

(Published in a Japanese version in the August 2012 issue of *Superconductivity Web 21*)

[Top of Superconductivity Web21](#)

Superconductivity Web21

Published by International Superconductivity Technology Center
1-10-13, Shinonome, Koto-ku, Tokyo 135-0062, Japan Tel: +81-3-3536-7283, Fax: +81-3-3536-5717

Feature Article: SQUID Applications - The Current Status of SQUID-Readout Development for Superconducting Detectors in Japan

Yoh Takei, Assistant Professor
Department of Space Astronomy and Astrophysics
Institute of Space and Astronautical Science
Japan Aerospace Exploration Agency

1. TES micro-calorimeter and SQUID

An attractive choice for applications requiring high precision is a cryogenic detector characterized by very low noise. An example of such a detector is a superconducting TES (transition-edge sensor) micro-calorimeter, which utilizes a highly sensitive thermometer that measures rapid resistance changes at the superconducting transition edge (Figure 1). The energy is measured for each detected X-ray photon. The spectroscopic performance is 50 times superior to a room-temperature semiconductor detector, realizing a resolution of 2 eV at 6 keV.

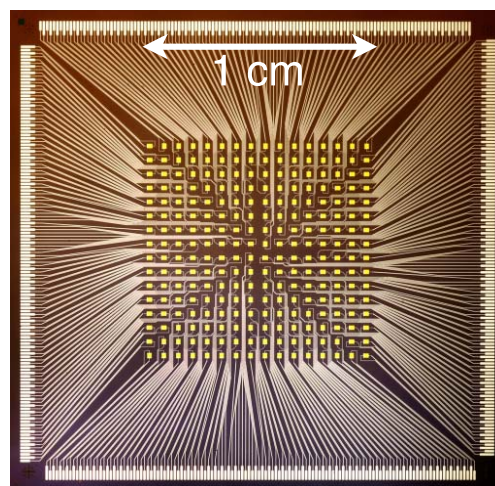
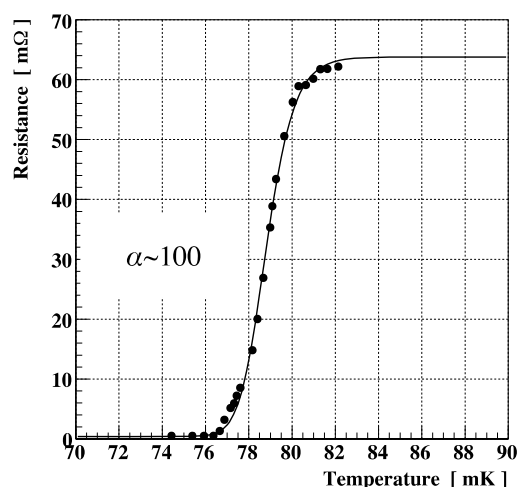


Fig.1 The relationship between resistance and temperature of a TES (left) and Photo of a 256-pixel TES micro-calorimeter array, fabricated by JAXA and Tokyo Metropolitan University ^{1),2)}

X-rays that hit a TES micro-calorimeter increase the resistance of the TES, which in turn change the current through it. Since the TES impedance is lower than 1Ω, an ammeter (preamplifier) with low impedance, high sensitivity and low noise is required to amplify and read out the signal. This is realized by a dc-SQUID magnetically coupled with the TES signal line via a superconducting coil. A TES and a SQUID is a good combination as they both utilize superconductors operating in a cryogenic environment. In fact, the significant progress in the development of the TES micro-calorimeters has only been achieved by combining a TES with a SQUID.

Superconductivity Web21

Published by International Superconductivity Technology Center
 1-10-13, Shinonome, Koto-ku, Tokyo 135-0062, Japan Tel: +81-3-3536-7283, Fax: +81-3-3536-5717

2. TES signal multiplexing realized with the development of a new SQUID

Both TES and SQUID development is key to realize practical TES micro-calorimeter applications. Particular applications are onboard-satellite applications observing X-rays from the universe. Here are strict limitations of power consumption and the amount of coolant available in orbit. We have been developing a SQUID that could enable signal multiplexing from several TES devices having lower dissipation in addition to sufficiently low noise and high gain. The fabrication of SQUIDs to meet these requirements has been undertaken using Nb standard process, based at the Superconductivity Research Laboratory, International Superconductivity Technology Center (ISTEC). Figure 2 shows the fabricated SQUID.

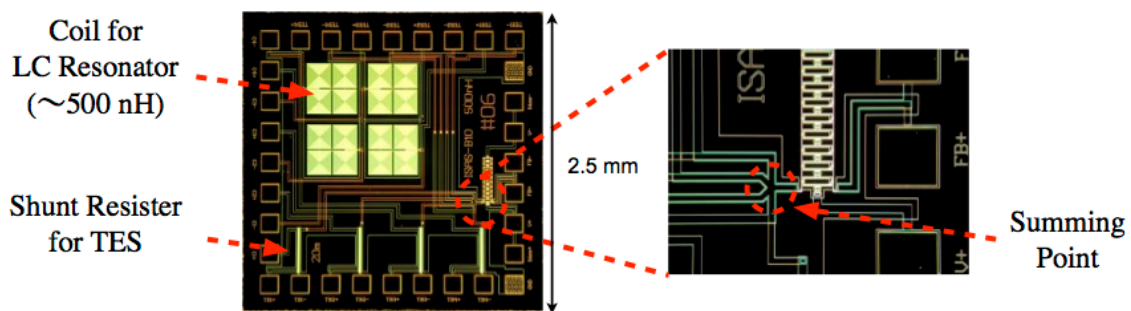


Fig. 2 Low heat dissipation/signal multiplexing SQUID developed in collaboration with ISTEC

For applications requiring the most advanced performance in the world, such as the space application field, the design and fabrication of SQUIDs has to match the characteristics of the detector developed. The collaboration with ISTEC is essential for us to develop and design devices using their facilities located in Japan that have excellent process capabilities. ISTEC's process line is able to fabricate and reproduce high quality JJs with small area, and hence is suitable for the development of high performance SQUIDs. The TES we are developing operates under an AC bias in a MHz band for the purpose of signal multiplexing. Thus, a TES shunt resistance and a superconducting coil for the LC bandpass filter are required. They are fabricated on the same chip as the SQUID device, as shown in Figure 2, allowing efficient use of the small chip space. Figure 3 shows examples of signals taken with the TES and the SQUID. This is the first successful simultaneous read-out of several TES signals operated at MHz bandwidths. It is pleasing that TES research has progressed significantly because of the SQUID development.

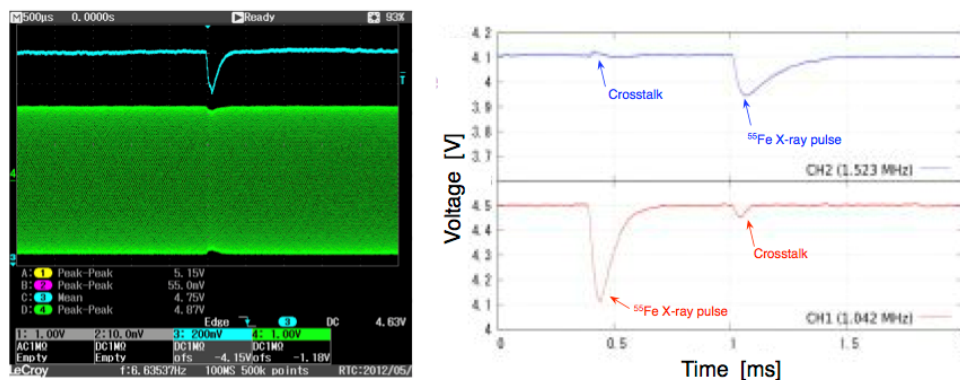


Fig. 3 Signal obtained with the combination of the developed TES and SQUID:
 Left: Feedback signal equivalent to SQUID signal input (green) and demodulated signal (blue),
 Right: Example of a demodulated signal from two TES devices operated at 1 and 1.5 MHz

Superconductivity Web21

Published by International Superconductivity Technology Center
1-10-13, Shinonome, Koto-ku, Tokyo 135-0062, Japan Tel: +81-3-3536-7283, Fax: +81-3-3536-5717

3. Conclusions

TES with high sensitivity and spectroscopic resolution has been utilized for not only X-ray astronomy but also for space applications at other wavelengths along with for microanalysis³⁾. Increasing TES pixel numbers and/or the capability for higher count rates are desirable for expanding the application with the TES micro-calorimeters. It is hoped that progress in SQUID development will lead to further advance in such applications in the future.

References:

1. Yuichiro Ezoe, Keisuke Shinozaki, Yoh Takei, Journal of the Physical Society of Japan, Vol. 64, Issue 8, p.61.
2. Ezoe *et al.*, 2009, AIP Conference Proc. 1185, 60.
3. <http://www.nims.go.jp/AEMG/recent/TES-TEM/TESTEM1006/TESTEM1006-1.html>

(Published in a Japanese version in the August 2012 issue of *Superconductivity Web 21*)

[Top of Superconductivity Web21](#)

Superconductivity Web21

Published by International Superconductivity Technology Center
1-10-13, Shinonome, Koto-ku, Tokyo 135-0062, Japan T el: +81-3-3536-7283, Fax: +81-3-3536-5717

Feature Article: Superconducting Digital Devices (Low Temperature) - Trends in Superconducting Digital Device Technology

Akira Fujimaki, Professor
Graduate School of Engineering
Nagoya University

The continuing trends of the eco-friendly generation have prompted superconducting digital circuits, which were previously considered as low-power consuming, to further reduce the power they consume. As introduced in my article published last year, logic circuits such as reciprocal quantum logic (RQL) produced by Northrop Grumman, energy-efficient rapid single flux quantum logic (ERSFQ) produced by Hypres and low-energy-consumption RSFQ (LE-RSFQ) produced by Nagoya University, all successfully reduced or completely eliminated power consumption caused by bias current supply resistance, which was the main draw of power in a conventional RSFQ circuit. Small and mid-size versions of these circuits have already been fabricated and their performance verified high-speed operations at more than several tens of GHz, and $1/10^{\text{th}}$ the power consumption compared to the conventional circuits.

Additionally, the eco-friendly generation has ignited once again the topic of Landauer, which asks '*what is the theoretical lower limit of energy consumption of computation for a classic logic circuit?*' This lower limit can be expressed as $kT \ln 2$ energy dissipated per irreversible bit operation. Discussions pertaining to the Landauer principle had been vigorous up until 25 years ago. However since there had been no technology available to verify this problem experimentally as well as the fact that low energy consumption led to low speed operation, the topic was not considered of prime research importance amongst scientists. It has once again become a topic on the agenda and recognized that the superconducting devices fabricated by enhanced fabrication technology allow the possibility to experimentally verify this conundrum. In response, Adiabatic Quantum Flux Parametron (A-QFP) and Negative SQUID (nSQUID) circuits have been proposed by Yokohama National University and Stony Brook University, respectively. These circuits offer the potential of operating at several GHz and comprise logic circuits that consume very little energy.

Since last year the trend for low power consumption has now spread to memory devices. For a computer its entire performance and power consumption is directly related to the performance/power consumption of its memory. High capacity memories with high speed/low power consumption characteristics matching the speed and power consumption of superconducting digital circuits are therefore required for constructing a superconducting computer offering greater performance and low power consumption characteristics. The USA has invited proposals to support projects to identify new candidate memory circuits that operate at low temperatures. Amongst the variety of topics include a large topic pertaining to the utilization of SFS Josephson Junctions with a ferromagnet (F) sandwiched between superconducting electrodes (S). The direction and strength of ferromagnet magnetization alters Josephson critical current values. The new memory device utilizes the ferromagnet as a storage medium and its contents are read out from the variation in critical currents. Originally an important concept in the operation of conventional superconducting memory was the ability for it to maintain quantum flux in a superconducting loop, however, this concept can be abandoned here. For example, Nagoya University has proposed that the concept of quantum flux memory be discarded, which implies that new memory devices have the potential of being compact and able to operate at far greater speeds than have been possible before. With the launch and

Superconductivity Web21

Published by International Superconductivity Technology Center
1-10-13, Shinonome, Koto-ku, Tokyo 135-0062, Japan T el: +81-3-3536-7283, Fax: +81-3-3536-5717

introduction of new physics, the author considers that superconducting digital devices have entered a completely new realm.

(Published in a Japanese version in the October 2012 issue of *Superconductivity Web 21*)

[Top of Superconductivity Web21](#)

Superconductivity Web21

Published by International Superconductivity Technology Center
1-10-13, Shinonome, Koto-ku, Tokyo 135-0062, Japan T el: +81-3-3536-7283, Fax: +81-3-3536-5717

Feature Article: Superconducting Digital Devices (Low Temperature) - The Fabrication Process Development of Small Al/AIO_x/Al Trilayer Josephson Junctions

Tetsuro Satoh, Senior Research Scientist
Low Temperature Superconducting Devices,
Electronic Devices Division,
SRL/ISTEC

Current general-purpose “classical” computers are slow for specific calculations such as factorization and discrete logarithms and it is practically impossible to process a large number of digits in such calculation, since an efficient algorithm has not been discovered. However, quantum computers on the other hand employ the quantum superposition, which is a principle of quantum mechanics for their operation, and it is highly expected much faster and more efficient parallel processing than computations performed by their “classical” counterparts.

In order for quantum computers to become reality their main components or quantum bits have to be realized. To address this, intensive worldwide research efforts are focusing on fundamental experiments to utilize a variety of physical systems such as trapped ions and semiconductor quantum dots as potential quantum bits. Amongst these, the integration and device characteristics of solid-state quantum bits are relatively easy to control and are therefore considered to have great engineering advantages in realizing a quantum computers. Superconducting circuits comprised of Josephson Junctions as solid-state quantum bits are one potential candidate.

Submicron-sized Josephson Junctions are required for superconducting quantum bits¹⁾. So far shadow evaporation method has been used for fabricating small junctions²⁾. However, in order for greater design flexibility in large scale integrated superconducting circuits, we need small junctions with trilayer geometry, which are based on a trilayer thin film of superconductor/tunnel barrier/superconductor. To this aim, we have been developing a fabrication process of Al/AIO_x/Al trilayer Josephson Junctions, which exhibits superior quantum bit characteristics, in collaboration with Innovation Center for Advanced Nanodevices, AIST.

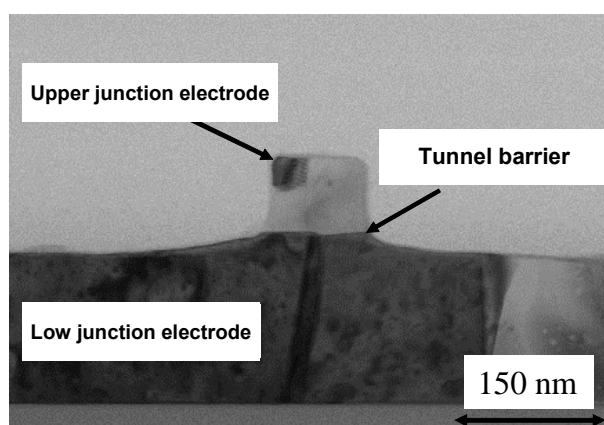


Fig. 1 Cross-sectional TEM image of junction pattern

Superconductivity Web21

Published by International Superconductivity Technology Center
1-10-13, Shinonome, Koto-ku, Tokyo 135-0062, Japan T el: +81-3-3536-7283, Fax: +81-3-3536-5717

The fabrication of small Al-based trilayer Josephson Junctions requires the formation of submicron-sized resist patterns and Al etching using the resist patterns as etch masks. We have thus been using electron beam lithography for forming small patterns together with a precise Al etching process utilizing Cl_2/BCl_3 -based reactive ion etching system. Figure 1 shows a cross-sectional TEM image of a junction pattern of 0.1 μm in diameter. We have successfully fabricated small junction patterns exhibiting steep sidewalls of more than 80° .

As trilayer junctions shrink to sub-micrometer dimensions, the fabrication of a superconducting contact formed in the upper part of the junction, as well as the fabrication of the junctions itself, become challenging. Usually this superconducting contact is formed by fabricating a via hole on the insulating layer attached to the junction, followed by depositing a superconducting layer on the sidewall of the via hole. However, the alignment of the via with the junction, the etching of the via, and the deposition of a superconducting layer on the via sidewalls are all difficult processes, in the case of submicron-sized junctions. To form the upper Junction contact, it is required to establish a process different to the conventional process. We have been therefore developing a process to form this upper superconducting contact by exposing the junction's upper electrode utilizing a planarization such as CMP.

Combined with the above-mentioned fabrication processes for small junctions with peripheral processes such as formation of contact, we have fabricated small Al trilayer junctions using this process. The characteristics of junctions of around 1 μm in diameter have been measured. Figure 2 shows the junction I-V characteristics measured at around 300 mK.

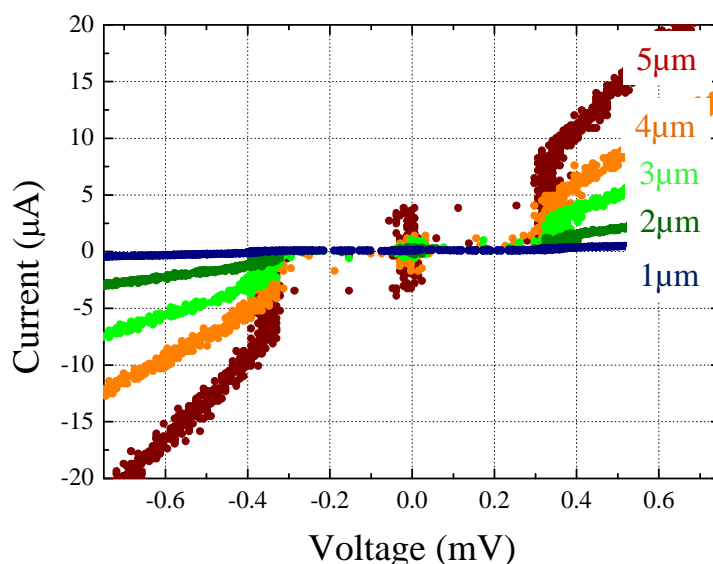


Fig. 2 I-V characteristics of Al trilayer junctions – measurement temperature at around 300 mK

The junction characteristics and their structural observation revealed that there is further room for improvement to optimize the contact formation process as well as cleaning process. We will solve such issues and fabricate submicron-sized junctions. Thus, we will fabricate and characterize superconducting quantum bits utilizing small Al trilayer junctions in the future.

Superconductivity Web21

Published by International Superconductivity Technology Center
1-10-13, Shinonome, Koto-ku, Tokyo 135-0062, Japan T el: +81-3-3536-7283, Fax: +81-3-3536-5717

Acknowledgements

This research is granted by the Japan Society for the Promotion of Science (JSPS) through the “Funding Program for World-Leading Innovative R&D on Science and Technology (FIRST Program),” initiated by the Council for Science and Technology Policy (CSTP).

References:

1. Jaw-Shen Tsai, Oyo Buturi, 78(2009),3.
2. G. J. Dolan, Appl. Phys. Lett., 31 (1977) 337.

(Published in a Japanese version in the October 2012 issue of *Superconductivity Web 21*)

[Top of Superconductivity Web21](#)

Superconductivity Web21

Published by International Superconductivity Technology Center
1-10-13, Shinonome, Koto-ku, Tokyo 135-0062, Japan T el: +81-3-3536-7283, Fax: +81-3-3536-5717

Feature Article: Superconducting Digital Device (LTS) - High Speed Operations of a Superconducting Flash A/D Converter in a Cryocooler System

Hideo Suzuki, Senior Research Scientist
Low Temperature Superconducting Device Laboratory,
SRL/ISTEC

A flash analog to digital (A/D) converter (also referred to as a Nyquist A/D converter) based on a superconducting SFQ circuit is a promising candidate because of its high speed characteristic with low power dissipation. It can also be constructed with low integration level than an equivalent semiconductor circuit by taking advantage of quantum phenomena. Principally, if a SFQ circuit is employed, then N-bit A/D converters can be constructed with N of comparators (On the other hand 2^N-1 of comparators are required for a semiconductor circuit). In a practical SFQ A/D converter, error correction is actually required to solve problems caused by thermal fluctuations and threshold fluctuations associated with slew rate in comparators (grey zone). A digital error correction method called as "look-back method" has been proposed as a potential solution¹⁾, and only the functional test of the error correction circuit had been performed. We have designed a fully integrated A/D converter with comparators and the error correction circuits, and then measured the operation with a high frequency.

ISTEC has been conducting R&D project aimed at high-speed A/D converters for optical communications, such as the next generation 100GbE, and future potential applications for waveform monitoring²⁾. Furthermore, a high speed A/D converter is expected in the future scientific applications such as digital signals conversion from the output of an array of superconducting sensors. This time, high frequency performance of a complimentary quasi-one-junction SQUID (CQOS) comparator, which was proposed by ISTEC, was improved in upgrading the design and fabrication process. The critical current density of Nb/AlOx/Nb junctions was increased to 10 kA/cm² (ISTEC STD3 process) from 2.5 kA/cm² (ISTEC STD2 process). The comparator was also reduced in size to improve the performance in a high-frequency. A prototype 5-bit A/D converter chip was designed and fabricated, in which the comparators and error correction circuits were both integrated in a 5mm-square chip

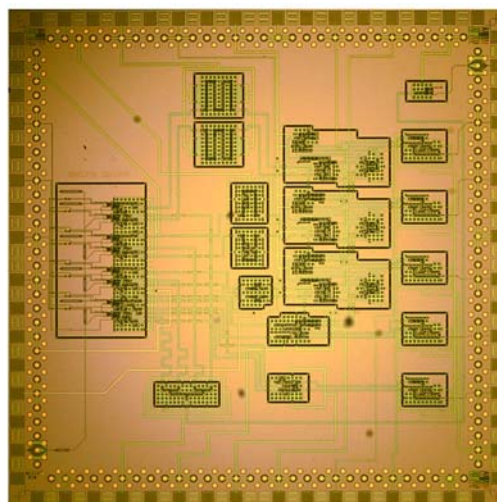


Fig. 1 A/D converter chip photo

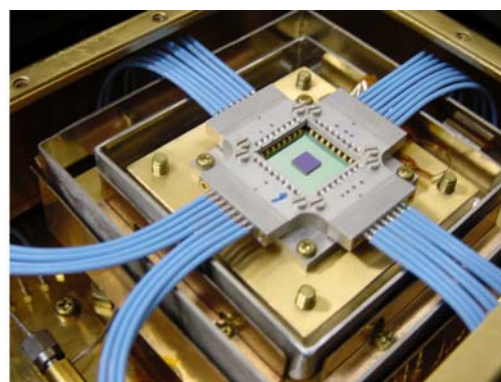


Fig. 2 A/D converter module attached onto 4 K refrigerator stage

Superconductivity Web21

Published by International Superconductivity Technology Center
1-10-13, Shinonome, Koto-ku, Tokyo 135-0062, Japan T el: +81-3-3536-7283, Fax: +81-3-3536-5717

(Figure 1). In order to perform a stable operation in a cryocooler system, we conceived an innovative technology in which a superconducting ground plane in a chip is locally isolated for each of component circuit blocks and they are connected to main ground plane with a finite resistance. This technological breakthrough avoids the influence of magnetic field due to bias return current to ground in the isolated circuits. This technology eliminated the bias current extraction³⁾, reducing the numbers of the input/output terminals in a cryocooler system. A cryopackage with 32-terminals (8-terminals X 4) with a 100GHz band-width was developed for the A/D converter and used for the demonstration equipped with a cryocooler system. An A/D converter chip was mounted onto this package after flip chip bonding to a 16mm-square MCM carrier. Figure 2 shows a micro-photograph when mounted to the 4K-cryocooler stage.

First, high frequency operations of the A/D converter was performed using a beat-frequency method (in this method, the input signal frequency is converted to a differential low frequency, Δf , between the signal frequency and the sampling frequency: set as $\Delta f=1$ kHz). The results confirmed around 4.5 bit operations and 3.5 bit operations at 10GHz and 15 GHz, respectively. Second, we successfully made experiments of A/D conversion with the introduction of a 10 GHz optical signal into the cooling system through an optical fiber. The optical signal was converted to electrical signal by a uni-traveling carrier photodiode (UTC-PD) operating at 4K. Third, a high frequency sampling operation was demonstrated with a 1 kHz low frequency signal input. A normal output waveform was observed with a sampling frequency of 100 GHz at 5 bit resolution, verifying high-speed clock operations for a SFQ circuit (Figure 3).

The A/D converter cooled by this cryocooler system had continuously operated for about 2 months without any trouble such as flux trapping.

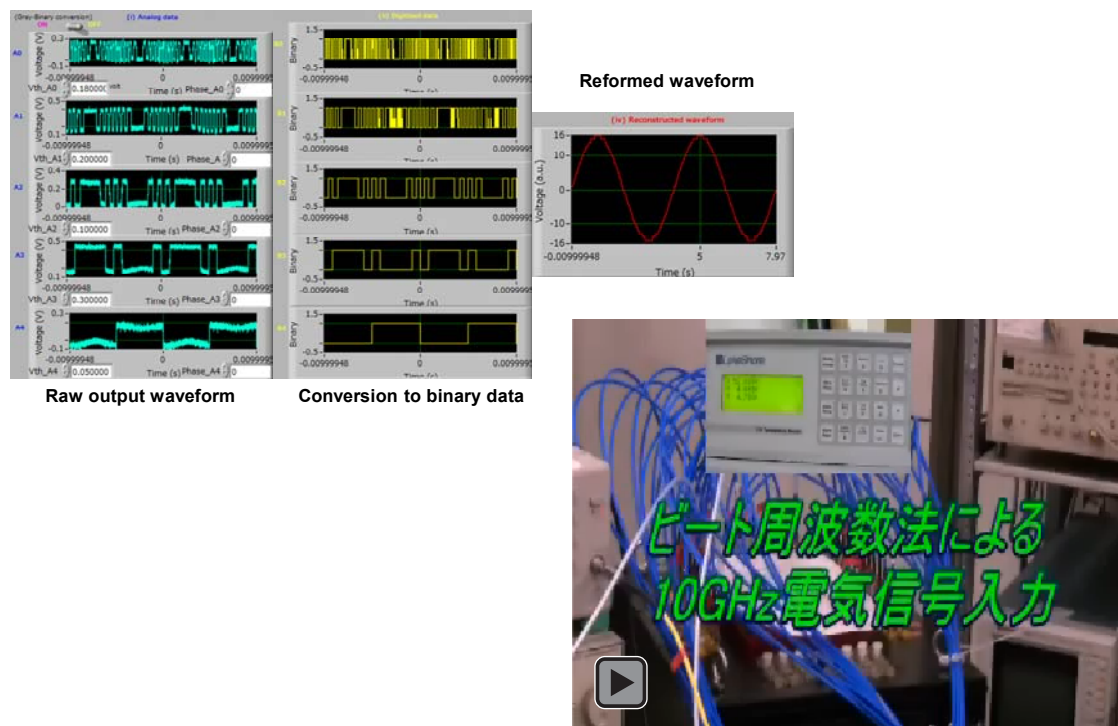


Fig. 3 Refrigerator operational waveforms produced at 100 GHz high speed sampling (input $f=1$ kHz) (left), movie (right)

Superconductivity Web21

Published by International Superconductivity Technology Center
1-10-13, Shinonome, Koto-ku, Tokyo 135-0062, Japan T el: +81-3-3536-7283, Fax: +81-3-3536-5717

This work was supported by the New Energy and Industrial Technology Development Organization (NEDO) as Development of Next-Generation High-Efficiency Network Device Project.

This work was partially supported by JSPS KAKENHI Grant Number 22226009.

References:

1. C. J. Anderson, IEEE Trans. Appl. Supercond., vol. 3, pp. 2769-2773, 1993.
2. S. B. Kaplan, et.al, IEEE Trans. Appl. Supercond., vol. 7, pp. 2822-2825, Jun. 1997.
3. Suzuki et al, Proceedings of the Society Conference of the Institute of Electronics, Information and Communication Engineers, C-8-5.

(Published in a Japanese version in the October 2012 issue of *Superconductivity Web 21*)

[Top of Superconductivity Web21](#)

Superconductivity Web21

Published by International Superconductivity Technology Center
1-10-13, Shinonome, Koto-ku, Tokyo 135-0062, Japan T el: +81-3-3536-7283, Fax: +81-3-3536-5717

Feature Article: Superconducting Digital Device (Low Temperature) - Investigation of Adiabatic QFP Logic Circuits with Extremely Low Power Consumption

Nobuyuki Yoshikawa, Professor
Department of Electrical and Computer Engineering
Graduate School of Engineering, Yokohama National University

In recent years the power consumption of high performance information equipment such as supercomputers and high-end servers has increased rapidly. However, their overall operating performance has been limited because of the heat generated. In particular, assuming an exa-scale supercomputer consumes a total of around 100 MW, and then its power supply alone constitutes upper limits on costs and facility capabilities of the system. In such circumstances, it is extremely difficult to reduce power consumption of future high performance information equipment by simply miniaturizing current CMOS integrated circuit devices. Therefore a radical reassessment on the calculation principles themselves needs to be considered to realize lower power consuming devices. Alternatively, developing a circuit consuming ultra-low power is strongly desired in the quantum-computing field to perform quantum feedback control at cryogenic temperatures.

A minimum energy threshold required for the calculation has long since been argued based upon thermodynamics and information theory undertaken in the past. Landauer et al predicted this limit to be $k_B T \ln 2$ per bit for an operation accompanying the erasure of information¹⁾. There have been arguments for and against this threshold but these have yet to be concluded. Nevertheless, experimental results supporting this threshold value have been recently reported²⁾.

Our research⁴⁾ has investigated the bit energy threshold of an adiabatically operating Quantum Flux Parametron (QFP)³⁾. Figure 1 shows comparisons of bit energies and gate delays between adiabatic QFP, RSFQ and CMOS logic circuits. It is clear to see that RSFQ operates at speeds several times greater than CMOS circuits, with around 3 orders of magnitude less power consumption. However, since a RSFQ circuit experiences non-adiabatic energy consumption, calculated as $I_c \Phi_0$ energy consumed for 1-bit operation. Here I_c is the Josephson Junction critical current value and Φ_0 is the flux quantum. On

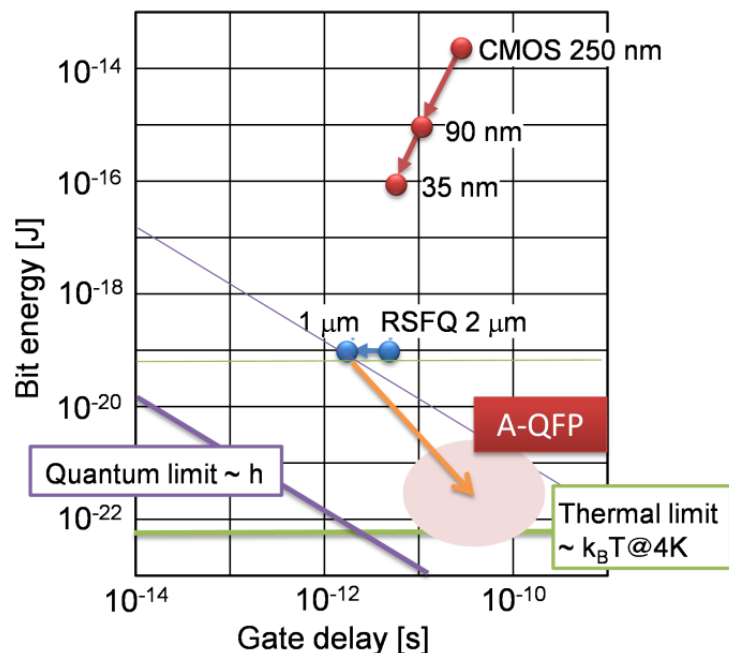


Fig. 1 Bit energy and gate delay of adiabatic-type QFP, RSFQ and CMOS logic circuit

Superconductivity Web21

Published by International Superconductivity Technology Center
 1-10-13, Shinonome, Koto-ku, Tokyo 135-0062, Japan T el: +81-3-3536-7283, Fax: +81-3-3536-5717

the other hand, an adiabatic QFP is designed to operate QFP at slow speeds in order to eliminate non-adiabatic energy consumption. Therefore, as a result, logic calculations of bit energies approaching $k_B T \ln 2$ are possible, as shown in Figure 1. Gate delays can be improved by enhancing the potential circuit speed by increasing the critical density of Josephson Junctions.

Figure 2 shows the operating principle of a QFP. A QFP comprises of a SQUID structure, with a shunt inductance and external magnetic field generated by exciting current. The excitation current modifies the QFP potential from a single-well to a double-well type. Firstly, the application of a small current input modifies the QFP potential from a single to a double-well, producing a transition state minimum value on either the left or right of the double-well potential. This corresponds to the invasion of single flux quanta to either the left or right superconducting loop. As a result, the output current (I_{out}) flows through the output inductance, the direction of which corresponds to the final state. An appropriate selection of junction parameters can eliminate all non-adiabatic energy consumption of a QFP and allow adiabatic operations⁴. Numerical calculations show that it is possible to reduce bit energies in a QFP down to 1 zJ whilst maintaining sufficient operating margins. Also, Monte Carlo simulation studies showed that sufficient operating margins could be sustained for operations down to 4.2 K⁵.

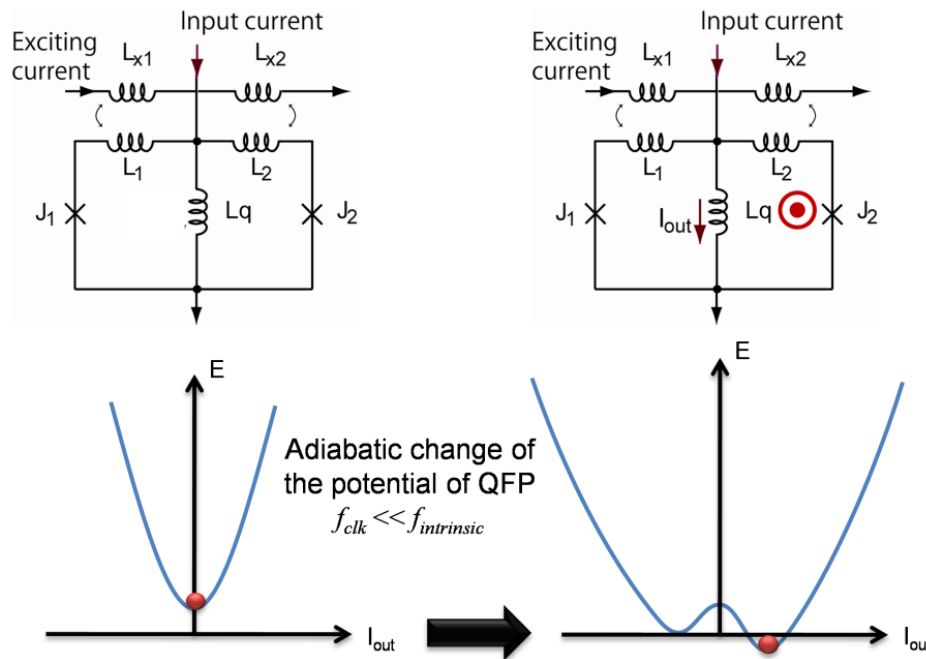


Fig. 2 Operating principle of adiabatic QFP

Figure 3 shows the circuit of a 1-bit full adder employing an adiabatic QFP, along with a photomicrograph. There were a total of 46 junctions, reducing by $\frac{1}{4}$ the number of junctions required compared to when a RSFQ circuit was used. Additionally, normal circuit operation was confirmed with low speed measurements and determined the exciting current operation margin to be $\pm 26.1\%$ ⁶.

Superconductivity Web21

Published by International Superconductivity Technology Center
1-10-13, Shinonome, Koto-ku, Tokyo 135-0062, Japan T el: +81-3-3536-7283, Fax: +81-3-3536-5717

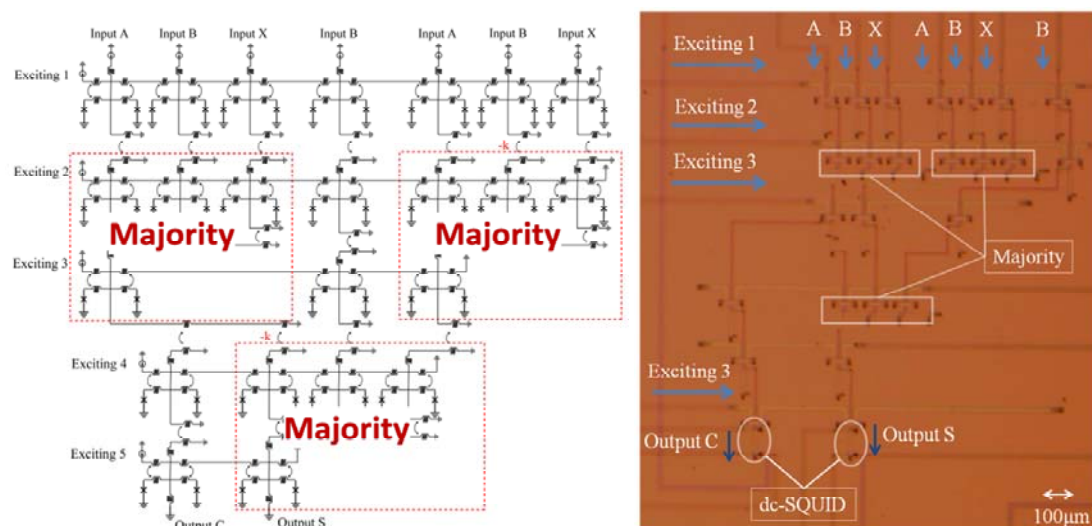


Fig. 3 Circuit diagram of a full adder utilizing adiabatic QFP (a), along with a photomicrograph (b)
The prototype circuit was fabricated utilizing ISTEK Nb Standard Process (STP2)

References:

1. R. Landauer, IBM J. Res. Develop. 5, 183 (1961).
2. A. Bérut, A. Arakelyan, A. Petrosyan, S. Ciliberto, R. Dillenschneider, and E. Lutz, Nature, 483, 187 (2012).
3. M. Hosoya, W. Hioe, J. Casas, R. Kamikawai, Y. Harada, Y. Wada, H. Nakane, R. Suda, and E. Goto, IEEE Trans. Appl. Supercond. 1, 77–89, (1991).
4. N. Yoshikawa, D. Ozawa, Y. Yamanashi, Extended Abstracts of the 2011 International Conference on Solid State Devices and Materials, September 2011, Nagoya, Japan.5.
5. N. Takeuchi, K. Ehara, K. Inoue, Y. Yamanashi and N. Yoshikawa, Accepted for publication in IEEE Trans. Appl. Supercond., (2013).
6. K. Inoue, K. Ehara, N. Takeuchi, Y. Yamanashi and N. Yoshikawa, Accepted for publication in IEEE Trans. Appl. Supercond., (2013).

(Published in a Japanese version in the October 2012 issue of *Superconductivity Web 21*)

[Top of Superconductivity Web21](#)

Superconductivity Web21

Published by International Superconductivity Technology Center
1-10-13, Shinonome, Koto-ku, Tokyo 135-0062, Japan Tel: +81-3-3536-7283, Fax: +81-3-3536-5717

Feature Article: Superconducting Digital Device (Low Temperature Superconductor) - Measurement of an SFQ Time to Digital Converter for Mass Spectrometry

Yuki Yamanashi, Associate Professor
Department of Electrical and Computer Engineering
Yokohama National University

Mass spectrometry is an analytical technique able to measure mass-to-charge ratio of a sample. In particular, conducting mass spectrometry of a high protein polymer is beneficial to identify complex structures and understand formation mechanisms. Thus, there are expectations that this method will evolve and lead to greater usage in the creation of new materials as well as an array of chemical and medical field applications. Time-of-flight mass spectrometry measures the mass-to-charge ratio of a molecule ionized using laser radiation and accelerated by a strong electric field, and subsequently measuring the time taken to reach a detector. Employing a superconducting strip detector (SSD) in time-of-flight mass spectrometry analysis allows precise determination of polymer protein composites, which would otherwise be impossible using time-of-flight measurements employing conventional detectors. Also, this new method allows distinction between molecules exhibiting similar mass-to-charge ratios. The research has therefore been progressing with an expectation that this method will open a new avenue of mass spectrometry applications.

SSDs exhibit higher detection speeds than conventional devices, however, in order to achieve an effective system capable of even greater operational speeds a SSD multi-array operating in parallel needs to be realized. This construction is effective for improving not only the detection speed but also the sample detection efficiency by enlarging the effective area of the SSD. However, currently available methods to simply construct SSD multi-arrays involve measuring SSDs, operating at a low temperature environment, by the system that is at room temperature. This gives rise to construction difficulties due to increasing thermal inflows as well as noise associated with the increase of cables. Thus, research has been advancing to build a system employing a superconducting single flux quantum (SFQ) circuit that operates at low temperatures. The figure below outlines a superconducting mass spectrometry system utilizing such an SFQ circuit. The current generated by an ion molecule detected by the multi-array SSD is converted to an SFQ voltage pulse that is digitally converted in the SFQ circuit. The SFQ voltage pulse is then input to the SFQ time-to-digital converter. The SFQ pulse input time is digitally measured with a resolution of several tens of picoseconds, thus enabling time-of-flight measurements to be undertaken with great precision. Also, since a SFQ circuit now measures all the SSDs, the number of cables connecting devices at low temperature to those at room temperature is drastically reduced, even for a multi-array arrangement.

We have developed a circuit consisting of a single SSD that converts an SSD signal to a digital SFQ pulse, enabling time-of-flight analysis to be performed on a sample. The likelihood of high precision mass spectrometry has been verified with the system developed. Future research will focus on the optimization of the entire system leading to construction of a multi-array of SSDs, capable of further precision mass spectrometry as well as fully taking advantage of the characteristics of SFQ circuits. Verifying detection efficiencies and imaging are planned.

Superconductivity Web21

Published by International Superconductivity Technology Center
1-10-13, Shinonome, Koto-ku, Tokyo 135-0062, Japan Tel: +81-3-3536-7283, Fax: +81-3-3536-5717

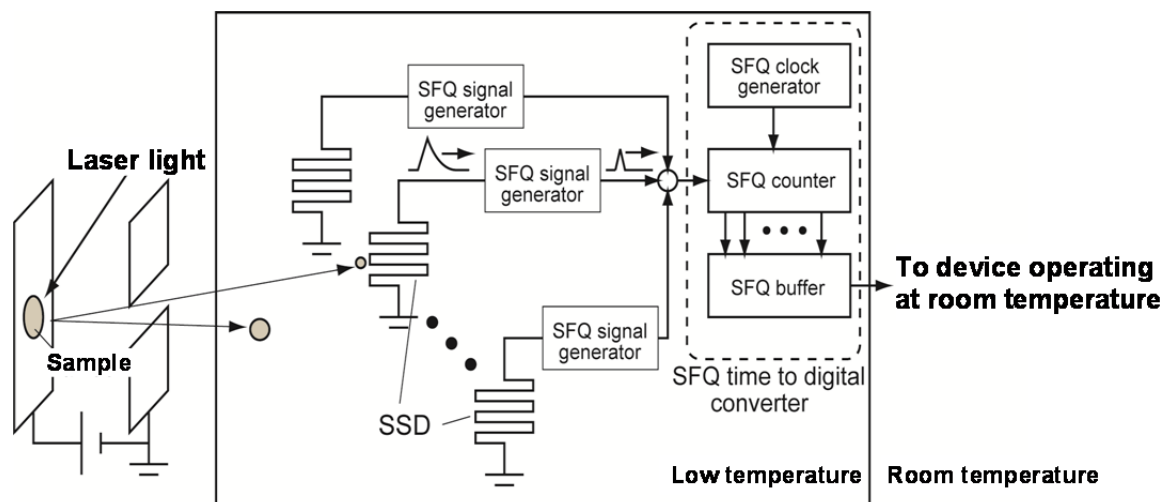


Fig. Schematic of the mass spectrometry system utilizing a superconducting single flux quantum (SFQ) circuit

(Published in a Japanese version in the October 2012 issue of *Superconductivity Web 21*)

[Top of Superconductivity Web21](#)

Superconductivity Web21

Published by International Superconductivity Technology Center
1-10-13, Shinonome, Koto-ku, Tokyo 135-0062, Japan T el: +81-3-3536-7283, Fax: +81-3-3536-5717

Feature Article: Superconducting Digital Device (Low Temperature) - Low-jitter Signal Readout from SSPD Utilizing A SFQ Circuit

Hiroataka Terai

Nano ICT Laboratory

National Institution of Information and Communication Technology

Superconducting single photon detectors (SSPD) have attractive features such as wide detectable wavelength range, high detection efficiency, high count rate, low dark-count rate and low timing jitter. It therefore draws attention as a potential photon detector, superior in performance characteristics over avalanche photodiodes (APD) and photomultiplier tubes (PMT). Of these features, low timing jitter is an especially important characteristic for many applications. For example, whilst quantum key distribution (QKD) systems have already attained a number of field test track records, pulse-position modulation on the other hand, has only been studied for communication applications such as optical links between satellites and space-to-ground communications. Furthermore, applications measuring spatial resolution for depth perception rely upon the time resolution of dark-field 3D imaging detectors and light detection and ranging (LIDAR) systems, therefore a detector with even greater detection efficiencies and low jitter characteristics is highly desirable.

The timing jitter of an SSPD increases inversely with the bias current, which can be easily understood by considering photon detection principles in a SSPD (e.g. Hotspot model). Additionally, the lack of sensitivity of a low noise amplifier also leads to larger jitter in readout electronics. These indicate that SSPDs with larger bias currents or larger critical current values give lower jitter characteristics. On the other hand, higher detection efficiencies are achievable using thinner superconducting films and narrower nano-wires. This implies that SSPDs with smaller critical current values are likely to have higher detection efficiencies. Thus, there is a conflict between realizing higher detection efficiencies and low jitter. High detection efficiencies and low jitter can be achievable by a low jitter signal readout utilizing a SSPD with small critical currents, which inevitably requires increased readout circuit sensitivity. We have focused on single flux quantum (SFQ) circuits as potential low jitter signal readout technology for SSPDs. This originates from earlier studies into the potential of SFQ circuits as a signal processing for an SSPD array¹⁾. An SSPD array allows higher count rates and photon-number-resolutions. However, thermal loads to refrigerator also increases because of the increased numbers of output cables required for a multi-element SSPD array. This can be resolved by processing the output signals in a cryogenic environment. We have proposed a SFQ signal

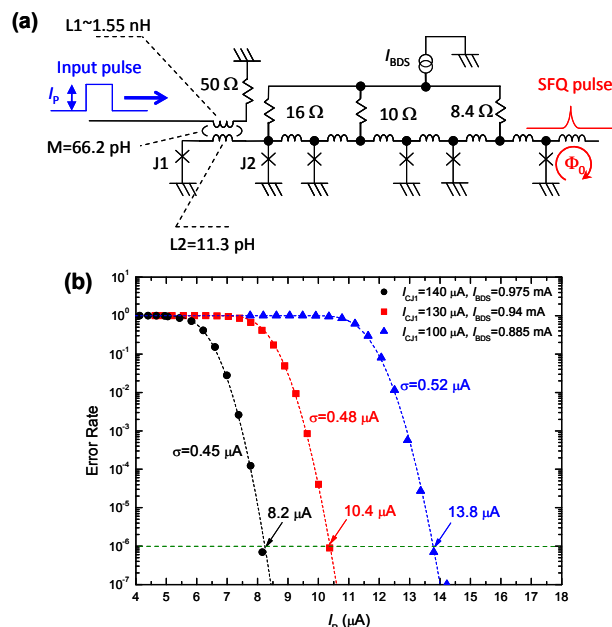


Fig. 1 The relationship between error rate and input current pulse strength of a SFQ readout circuit

Superconductivity Web21

Published by International Superconductivity Technology Center
1-10-13, Shinonome, Koto-ku, Tokyo 135-0062, Japan T el: +81-3-3536-7283, Fax: +81-3-3536-5717

processing circuit designed for SSPD arrays¹⁾ and have verified signal readout operations from SSPDs utilizing SFQ circuits^{2),3)}. Furthermore, crosstalk-free operations of a four-pixel SSPD array, including signal processing, utilizing SFQ circuit have been successfully demonstrated⁴⁾. However, we have not demonstrated the advantages of SFQ readout circuits in respect of timing jitter, because the previous readout circuit was designed to achieve a wide operating margin rather than a high current sensitivity. Low jitter signal readout from a SSPD can be realized by further enhancing the input current sensitivity since a SFQ circuit itself operates at a low jitter of 0.1 ps per Josephson junction. Circuit parameter re-optimization has been reassessed this time and focused on current sensitivity to verify low-timing jitter signal readout from a SSPD⁵⁾. To convert a small signal from the SSPD to an SFQ pulse, a magnetic transformer has been installed at the circuit input. Figure 1(a) shows an equivalent SSPD-SFQ converter circuit. An increase in the numbers of windings in transformer coil improves current sensitivity, but there is a trade off with input signal bandwidths. In this experiment, the magnetic transformer was designed the same as a conventional circuit but other circuit parameters were optimized, which produced current sensitivity improvements. The results showed that input current sensitivity significantly depended on the critical current values of Josephson junction J1 included in the washer coil in magnetic transformer. Figure 1(b) shows the dependency between the input current pulse amplitude of the SFQ readout circuit and the error rate. By increasing J1 to 140 μA from 100 μA of a conventional circuit, the input current sensitivity (defined as the input current pulse amplitude giving error rate of 10^{-6}) was improved to 8.2 μA from 13.8 μA observed in conventional circuit. The timing jitter of the SFQ readout circuit was also measured utilizing a pulse pattern generator (PPG) and a time-correlated single-photon counting (TCSPC) module with a 1 ps time resolution. The experimental setup for jitter measurements is shown in Figure 2(a). This experimental setup is quite similar with that for the jitter measurement of SSPD, but a femto-second laser and the SSPD are replaced by the PPG and the SFQ circuit, respectively. The jitter was calculated from the full-width-at-half-maximum histogram output peak count acquired by the TCSPC module. The results are shown in Figure 2(b). In the circuit with the critical current of J1 of 140 μA , the SFQ readout circuit jitter kept constant at around 30 ps for the input pulse current value was more than 15 μA . In order to reveal the origin of residual jitter at 30 ps, the SFQ circuit was removed in the experimental setups shown in Figure 2(a). The results are shown in the inset of Figure 2(b). When the input voltage to the low noise amplifier was set at 2 mV, which corresponds to the output voltage of the SFQ circuit, the observed jitter was around 30 ps. Therefore, this indicates that the residual 30 ps jitter comes from the experimental setup, and the measured timing jitter of SFQ readout circuit was much lower than 30 ps at an input pulse current value of more than 15 μA . It therefore concluded that we could not measure using this experimental setup.

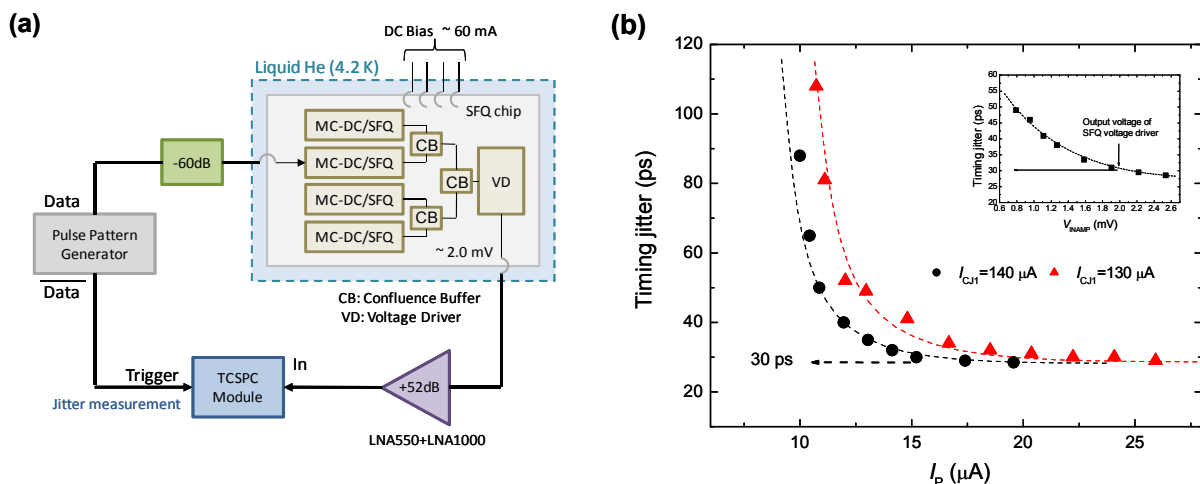


Fig. 2 (a) Jitter measurement system employing a SFQ circuit, (b) Jitter measurement results obtained using a SFQ circuit

Superconductivity Web21

Published by International Superconductivity Technology Center
1-10-13, Shinonome, Koto-ku, Tokyo 135-0062, Japan T el: +81-3-3536-7283, Fax: +81-3-3536-5717

Then the SSPD and SFQ readout circuit were implemented onto a 0.1W GM (Gifford-McMahon) and the timing jitter was measured. Experimental measurements were performed with a SSPD at a critical current of around $18 \mu\text{A}$ and a detection efficiency of 16 % at a dark-count rate, of 100 Hz. Prior to measuring the timing jitter using SFQ readout circuit, the timing jitter was measured using a conventional readout. The experimental setup with the SFQ readout circuit is shown in Figure 3(a). We have already confirmed that the bias current dependency of the detection efficiency measured using the setup shown in Figure 3(a) well agrees with the results obtained by conventional measurements³⁾. The results are shown in Figure 3(b). In conventional methods without the SFQ readout circuit, the 50Ω resistor is usually connected to the SSPD in parallel, and acts as an escape path for the bias current to the SSPD (I_{SSPD}) when the SSPD goes into a resistive state known as “latching.” The effect of the 50Ω resistor is clearly seen in Figure 3(b). The upper limit of I_{SSPD} is about $18 \mu\text{A}$ for the SSPD with the parallel shunt, and as large as $14.5 \mu\text{A}$ without the parallel shunt. During practical use of the SSPD, the 50Ω shunt resistor is thus indispensable for achieving as high a DE as possible. However, the parallel shunt also makes the input current of the LNA half of I_{SSPD} , causing an increase of the timing jitter. With the 50Ω parallel shunt, the jitter was around 67ps at a bias current of $18 \mu\text{A}$. When a SFQ readout circuit was connected, the measured jitter was approximately 37 ps, confirming the significant reduction in jitter. There is no need for the 50Ω shunt resistance when connecting the SFQ circuit directly to the SSPD without bias tees (50Ω termination resistance at SFQ circuit side has a parallel shunt effect). This is far superior compared to conventional readout methods utilizing bias tees and low-noise amplifier operating at room temperature. Further, a timing jitter of 37 ps could not be achieved by the conventional readout without the 50Ω shunt even if I_{SSPD} could be increased to $18 \mu\text{A}$. Therefore, the SFQ readout circuit offers a great advantage for achieving a low-jitter signal readout from the SSPD while keeping the DE as high as possible..

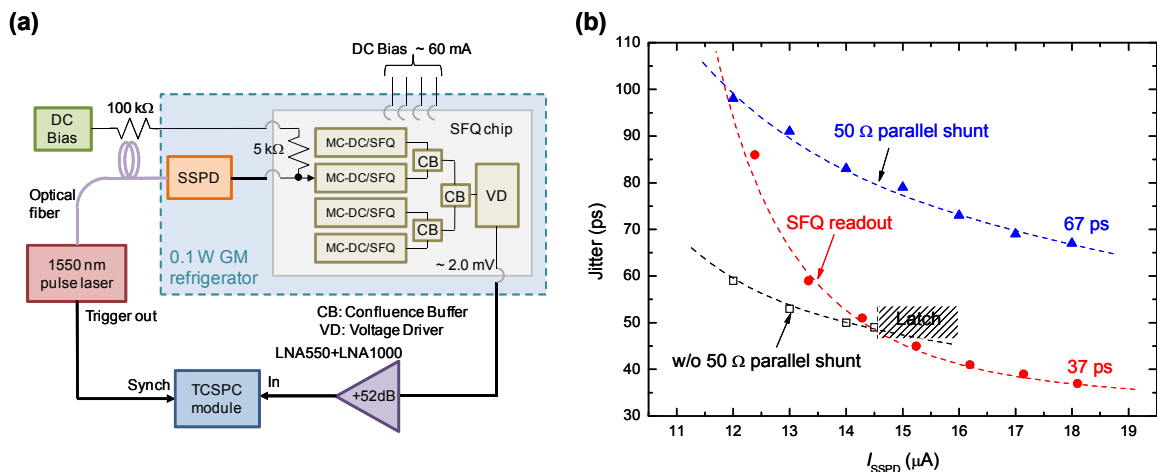


Fig. 3 (a) SSPD jitter measurement utilizing SFQ readout circuit, (b) Comparisons of jitter between a conventional readout and a SSPD employing an SFQ readout

These findings imply that SFQ readout circuits are beneficial not only as signal processing circuits to realize SSPD arrays, but also to realize low jitter signal readouts. There will be further opportunities to utilize SFQ readout circuits for the purpose of jitter reduction in various applications.

Reference:

1. Terai, S. Miki, and Z. Wang, IEEE Trans. on Appl. Supercond., Vol. 19, 350, 2009.

Superconductivity Web21

Published by International Superconductivity Technology Center
1-10-13, Shinonome, Koto-ku, Tokyo 135-0062, Japan T el: +81-3-3536-7283, Fax: +81-3-3536-5717

2. Terai, S. Miki, T. Yamashita, K. Makise, and Z. Wang, Appl. Phys. Lett., Vol. 97, 112510, 2010.
3. S. Miki, H. Terai, T. Yamashita, K. Makise, M. Fujiwara, M. Sasaki, and Z. Wang, Appl. Phys. Lett., Vol. 99, 111108, 2011.
4. T. Yamashita, S. Miki, H. Terai, K. Makise, and Z. Wang, Opt. Lett. Vol. 37, 2982-2984 (2012).
5. H. Terai, T. Yamashita, S. Miki, K. Makise, and Z. Wang, Opt. Express Vol. 20, 20115-20123 (2012).

(Published in a Japanese version in the October 2012 issue of *Superconductivity Web 21*)

[Top of Superconductivity Web21](#)

Superconductivity Web21

Published by International Superconductivity Technology Center
 1-10-13, Shinonome, Koto-ku, Tokyo 135-0062, Japan T el: +81-3-3536-7283, Fax: +81-3-3536-5717

Feature Article: Superconducting Digital Devices (Low Temperature) - Success in a Principle Experiment Related to Quantum Memory – Advancement towards The Realization of A Quantum Computer

Shiro Saito
 Senior Research Scientist
 NTT Basic Research Laboratories
 Nippon Telegraph and Telephone Corporation

1. Introduction

Recently worldwide attention has focused upon potential qubit candidates, a quantum state of a two-level system, for quantum computation and information processing applications. In particular, intensive research efforts on superconducting qubits have been conducted, leading to expectations of superior controllability due to it being an artificial atom (a macroscopic quantum system), and future scalability related to a greater degree of freedom in the design of superconducting circuits. Recent exploits have thus far realized quantum operations and quantum circuits/processes utilizing several qubits ^{1),2)}, with coherence times now up to 0.1 milliseconds. Such coherence times have increased by 5 orders of magnitude over the last ten years ^{3),4)}. However, despite these advances there is still a significant lag in these coherence times compared with those of electron and nuclear spins of natural microscopic quantum system. Recent research efforts have focused on utilizing an electron spin ensemble as a potential quantum memory for a superconducting-based qubit ^{5),6)}.

As potential candidates for quantum memories our research has been progressing with a focus on the electron spins present in negatively charged nitrogen-vacancy centers (NV) in a diamond crystal (see Figure 1). This article introduces a proof of principle experiment conducted to validate the characteristics of a superconductor/diamond hybrid quantum system ⁷⁾.

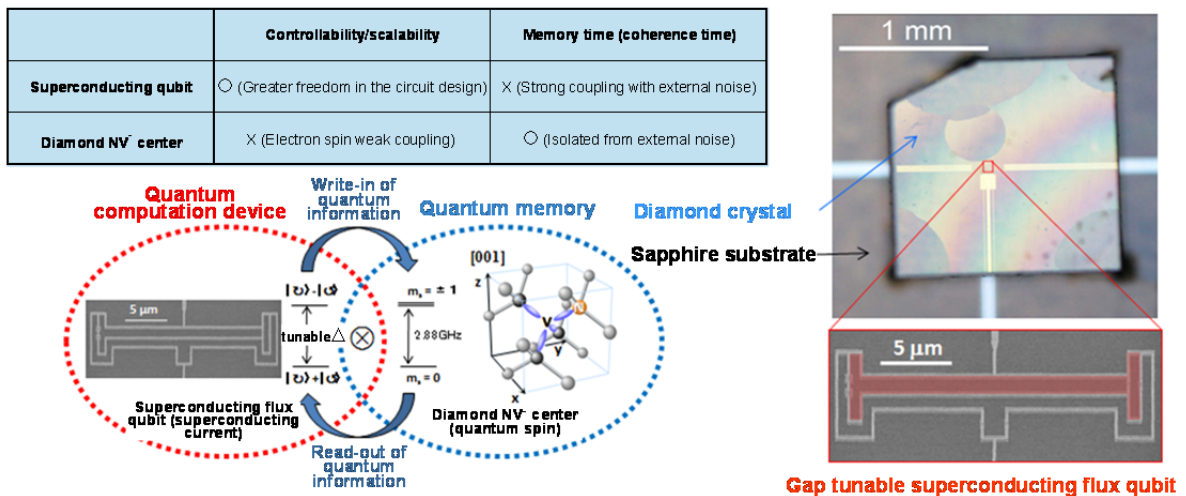


Fig. 1 A superconductor/diamond hybrid quantum system

Superconductivity Web21

Published by International Superconductivity Technology Center
1-10-13, Shinonome, Koto-ku, Tokyo 135-0062, Japan T el: +81-3-3536-7283, Fax: +81-3-3536-5717

2. Preparation of NV centers in diamond and the superconducting flux qubit

The electron spin of NV centers in diamond crystal is a spin 1 system which possesses a 2.88 GHz zero field ground state splitting. We have developed a gap tunable superconducting flux qubit where one can tune the splitting of the energy gap (Δ) as required⁸⁾. Additionally, diamond crystals containing high-density NV centers were prepared to realize strong coupling between the two systems. The natural coupling between a single electron spin and the flux qubit is relatively small at 8.8 kHz. However by using collective effects it can be increased by \sqrt{N} (where N is the number of NV centers). A superconductor/diamond hybrid system was fabricated by pasting a prepared diamond crystal carefully onto a qubit sample fabricated on a sapphire substrate (Figure 1 Photo).

3. Experimental results of hybrid system

The measurements have all been undertaken using a dilution refrigerator set at a base temperature of ~ 12 millikelvin. The qubit flux sample with attached diamond crystal had an observed energy splitting of 70 MHz at its minimum energy, as determined by microwave spectroscopy (Figure 2(a)). The 2.878 GHz center splitting frequency coincided well with the zero field splitting of an NV center. We however did not observe any splitting in previous spectroscopy studies where the diamond sample was not attached (Figure 2(a) inset). This lead to the conclusion that the observed splitting was attributed to a Vacuum Rabi splitting, produced by a strong coherent coupling of the flux qubit to the electron spin ensemble within diamond. Also, by considering the splitting width, the number of electron spins that couple coherently with the flux qubit was estimated to be several tens of millions.

Additionally, time-domain experiments were performed in order to verify quantum memory operations. Whilst the flux qubit and the electron spin ensemble are detuned sufficiently, it is only the qubit that was excited to a higher state with the application of a microwave pulse. A rapid change in the energy of the qubit leads to resonance within the spin ensemble. However, this time, the energy changes far more rapidly than that observed with Vacuum Rabi splitting, generating a non-adiabatic transition that leads to Vacuum Rabi oscillations, which imply that the flux qubit coherently exchanges a single quantum of energy with the spin ensemble (Figure 2(b)). This vibration exactly coincides with the repeated write-in and read-out of quantum information from a qubit to a spin ensemble.

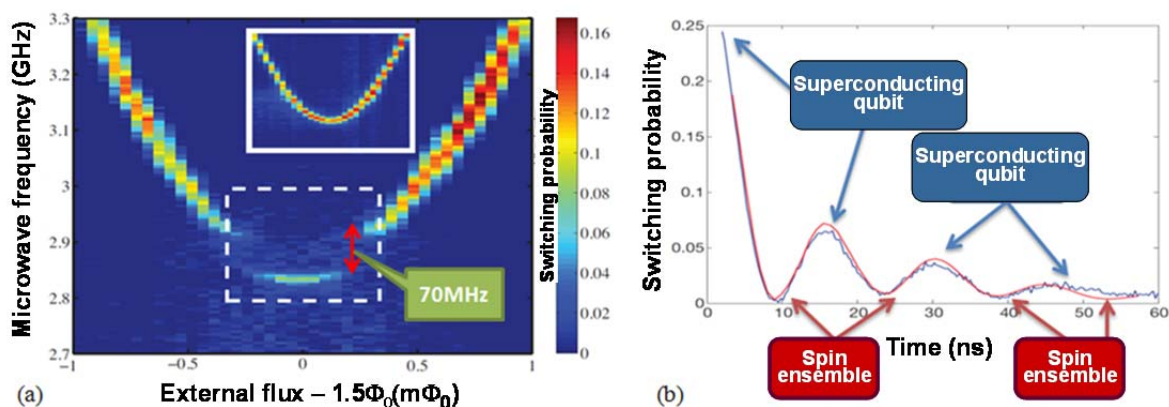


Fig. 2 (a) Microwave spectroscopy, (b) Vacuum Rabi oscillations between a superconducting qubit and a spin ensemble

Superconductivity Web21

Published by International Superconductivity Technology Center
1-10-13, Shinonome, Koto-ku, Tokyo 135-0062, Japan T el: +81-3-3536-7283, Fax: +81-3-3536-5717

4. Conclusions

The coherent quantum coupling between an electron spin ensemble of NV⁻ centers within diamond and a superconducting flux qubit have been observed successfully. These findings imply that it is possible to continuously write-in and read-out the quantum information from the superconducting qubit to the spin ensemble within a diamond crystal. We thus propose that diamond would be an extremely promising candidate in order to realize a quantum memory, a necessity for quantum communications as well as general quantum information processing.

This research was undertaken in cooperation with Osaka University and the National Institute of Informatics. This work was supported in part by the Funding Program for World-Leading Innovative R&D on Science and Technology (FIRST), a Grant-in-Aid for Scientific Research on Innovative Areas (grant no.22102502), a Scientific Research (A) grant no. 22241025 from the Japanese Society for the Promotion of Science (JSPS), and a grant from the National Institute of Information and Communications Technology (NICT).

References:

1. M. D. Reed, *et al.*, Nature 482, 382 (2012).
2. M. Neeley, *et al.*, Nature 467, 570 (2010).
3. Y. Nakamura, Y. A. Pashkin, and J. S. Tsai, Nature 398, 786 (1999).
4. C. Rigetti, *et al.*, Phys. Rev. B 86, 100506(R) (2012).
5. D. Marcos, *et al.*, Phys. Rev. Lett. 105, 210501 (2010).
6. Y. Kubo, *et al.*, Phys. Rev. Lett. 105, 140502 (2011).
7. X. Zhu, *et al.*, Nature 478, 221 (2011).
8. X. Zhu, *et al.*, Appl. Phys. Lett. 97, 102503 (2010).

(Published in a Japanese version in the October 2012 issue of *Superconductivity Web 21*)

[Top of Superconductivity Web21](#)